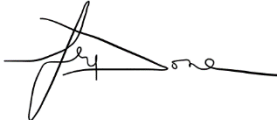




Technical Note on Quality Assessment for Jilin-1 KF01 (Earth Scanner)

Author(s): 

Fay Done
Task 1 Mission Expert

Approval: 

Fay Done
Task 1 Lead

Accepted: 

Clement Albinet
EDAP Technical Officer

TABLE OF CONTENTS

1. INTRODUCTION	4
1.1 Reference Documents	4
1.2 Glossary	6
2. EXECUTIVE SUMMARY	7
3. EDAP QUALITY ASSESSMENT	10
3.1 EDAP Maturity Matrix.....	10
3.1.1 Product Information	11
3.1.2 Product Generation.....	14
3.1.3 Ancillary Information	15
3.1.4 Uncertainty Characterisation	16
3.1.5 Validation	17
4. DETAILED Jilin-1 KF01 QUALITY ASSESSMENTS	19
4.1 Objectives	19
4.2 Geometric Calibration Quality	19
4.2.1 Absolute Geolocation Accuracy.....	19
4.2.1.1 Description and Method I (Panchromatic)	19
4.2.1.2 Results I	20
4.2.1.3 Description and Method and II (Multispectral)	22
4.2.1.4 Results II	23
4.2.2 Temporal Geolocation Accuracy	24
4.2.3 Band Co-registration Accuracy.....	24
4.2.3.1 Description and Method	24
4.2.3.2 Results	24
4.3 Radiometric Calibration Quality.....	26
4.3.1 Absolute Radiometric Accuracy.....	27
4.3.1.1 Description and Method	27
4.3.1.2 Results	28
4.3.2 Temporal Radiometric Accuracy	30
4.4 Image Quality	30
4.4.1 Signal-to-Noise Ratio	31
4.4.1.1 Description and Method	31
4.4.1.2 Results	32
4.4.2 Modulation Transfer Function	35
4.4.2.1 Description and Method	35
4.4.2.2 Results	37
4.4.3 Image Interpretability	40
4.4.3.1 Description and Method	40
4.4.3.2 Results	42
4.5 Visual Inspections	54
4.5.1 Description and Method	54
4.5.2 Results	54
5. CONCLUSIONS	58
APPENDIX A GSD ASSESSMENT	59
APPENDIX B MTF	60
APPENDIX C Jilin-1 KF01A/B TEST DATASET	61

AMENDMENT RECORD SHEET

The Amendment Record Sheet below records the history and issue status of this document.

ISSUE	DATE	REASON
0.1	21 01 2022	First draft for ESA review
1.0	23 06 2022	Final issue

1. INTRODUCTION

This technical note details the results of the preliminary data quality assessments (geometric calibration, radiometric calibration and image quality) performed on a sample of orthorectified bundle products generated for the optical Earth Observation (**EO**) **Jilin-1 KF01A and B** (“**Earth Scanner**”) missions.

The aforementioned data quality assessments are performed in accordance with the assessment guidelines, detailed in [RD-1, RD-2], that constitute the European Space Agency (**ESA**) Earthnet Data Assessment Pilot (**EDAP**) Project’s *EO Mission Data Quality Assessment Framework*. An important representation of the latter framework, constructed by the National Physical Laboratory (**NPL**), is what is known as the *maturity matrix*. It is a diagrammatic summary of the following:

- **Documentation Review:** *the EDAP optical team reviews materials provided by the data provider and / or operator (e.g. ancillary / auxiliary data and documentation), some of which may not be publicly available, and the scientific community (e.g. published papers). The results are detailed in Section 3 (covering the first four columns of the maturity matrix, see Table 3-1).*
- **Data Quality Assessments:** *the EDAP optical team performs data quality assessments (i.e. validation assessments), independently of those performed by the data provider and / or operator. The results are detailed in Section 4 (covering the last column of the maturity matrix, see Table 3-1).*

The above data quality assessments are performed by the project’s optical team using the appropriate in-house and open-source ad-hoc scripts / tools.

It is important to note the purpose of the *EDAP EO Mission Data Quality Assessment Framework* is to ensure the delivered commercial mission data (products) is fit for purpose and that all decisions regarding the inclusion of the commercial mission as an ESA third party mission can be made fairly and with confidence.

1.1 Reference Documents

The following is a list of reference documents with a direct bearing on the content of this proposal. Where referenced in the text, these are identified as [RD-n], where 'n' is the number in the list below:

- RD-1. EDAP Best Practice Guidelines, EDAP.REP.001, v1.2, September 2019.
- RD-2. Earth Observation Mission Quality Assessment Framework – Optical Guidelines, EDAP.REP.002, v2.0, December 2020.
- RD-3. Chang Guang Satellite Technology Co Ltd. - Jilin-1 Imagery Product Guide, v1.1, April 2021.
- RD-4. Head Aerospace – Introduction to the Jilin-1 Satellites and Products, v0.1 (Draft), May 2020.
- RD-5. Jilin-1 Satellites Radiometric Calibration (not publicly available and no other document information provided)

- RD-6. Wilkinson, M.D., Dumontier, M., Aalbersberg, I.J., Appleton, G., Axton, M., et al. 2016 The FAIR Guiding Principles for scientific data management and stewardship. *Scientific Data* 3, 160018. (doi:10.1038/sdata.2016.18)
- RD-7. Head Aerospace - Earth Scanner (JL-1 KF01) Data Sheet, v1.0, 2020.
- RD-8. Bouvet, M.; Thome, K.; Berthelot, B.; Bialek, A.; Czapla-Myers, J.; Fox, N.P.; Goryl, P.; Henry, P.; Ma, L.; Marcq, S.; Meygret, A.; Wenny, B.N.; Woolliams, E.R. RadCalNet: A Radiometric Calibration Network for Earth Observing Imagers Operating in the Visible to Shortwave Infrared Spectral Range. *Remote Sens.* 2019, 11, 2401, <https://doi.org/10.3390/rs11202401>
- RD-9. M. Cournet, A. Giros, L. Dumas, J.M. Delvit., D. Greslou, F. Languille, G. Blanchet, S. May, and J. Michel (2016). 2D Sub-Pixel Disparity Measurement Using QPEC / Medicis, Int. Arch. Photogramm. Remote Sens. Spatial Inf. Sci., XLI-B1, 291-298, doi: 10.5194/isprs-archives-XLI-B1-291-2016.
- RD-10. John Pike, National Image Interpretability Scale. 1998, <https://fas.org/irp/imint/niirs.htm> Accessed online: 22 October 2021
- RD-11. Zaroni, "IKONOS Signal-to-Noise Ratio Estimation", March 25-27, 2002, JACIE Workshop, 2002 <https://ntrs.nasa.gov/search.jsp?R=20040004380>
- RD-12. Françoise Viallefont-Robinet, Dennis Helder, Renaud Fraisse, Amy Newbury, Frans van den Bergh, Donghan Lee, Sébastien Saunier. Comparison of MTF measurements using edge method: towards reference data set. *Optics Express*, Optical Society of America, 2018, 26 (26), pp.33625-33648. (hal-02055611)
- RD-13. Chang Guang Satellite Technology Co., Jilin-1 KF01A (http://www.charmingglobe.com/EWeb/product_view.aspx?id=682)
- RD-14. Blanc, P., Wald, L. 2009, A review of earth-viewing methods for in-flight assessment of modulation transfer function and noise of optical spaceborne sensors, https://www.researchgate.net/publication/259157057_A_review_of_earth-viewing_methods_for_in-flight_assessment_of_modulation_transfer_function_and_noise_of_optical_spaceborne_sensors
- RD-15. SPOT Image Quality Performances, CNES C443-NT-0-296-CN, https://www.intelligence-airbusds.com/files/pmedia/public/r438_9_spot_quality_performances_2013.pdf
- RD-16. Teke, M. A Simple GSD Analysis of Earth Observation Systems, January 2019, <https://mustafa-teke.medium.com/a-simple-gsd-analysis-of-earth-observation-systems-cc1119fac530>
- RD-17. Sentinel-2 MPC L1C Data Quality Report, S2-PDGS-MPC-DQR, Issue 71, 03/01/2022. https://sentinel.esa.int/documents/247904/685211/Sentinel-2_L1C_Data_Quality_Report
- RD-18. Department of the Interior U.S. Geological Survey, Landsat 8 (L8) Data Users Handbook, L8SDS-1574, Version 5.0, <https://prd-wret.s3-us-west->

2.amazonaws.com/assets/palladium/production/atoms/files/LSDS-
1574_L8_Data_Users_Handbook-v5.0.pdf

1.2 Glossary

The following acronyms and abbreviations have been used in this Report.

ATBD	Algorithm Theoretical Basis Document
BRDF	Bidirectional Reflectance Distribution Function
CAMS	Copernicus Atmospheric Monitoring Service
CEOS	Committee for Earth Observation Satellites
DEM	Digital Elevation Model
EDAP	EARTHNET Data Assessment Pilot
FAIR	Findable, Accessible, Interoperable and Reusable
GCP	Ground Control Points
GPS	Global Positioning System
IVOS	Infrared and Visible Optical Sensors, Infrared and Visible Optical Sensors
MS	Multispectral
MSI	Multispectral Instrument
MTF	Modulation Transfer Function
NIIRS	National Imagery Interpretability Rating Scale
NPL	National Physical Laboratory
PAN	Panchromatic
PICS	Pseudo-Invariant Calibration Site
SNR	Signal-to-Noise Ratio
VHR	Very High Resolution
WGCV	Working Group for Calibration and Validation

2. EXECUTIVE SUMMARY

The Jilin-1 constellation of EO satellites, developed and operated by **Chang Guang Satellite Technology** (China), consists of the optical **Jilin-1 KF01 (“Earth Scanner”) A** (launched January 2020) and **B** (launched September 2021) twin satellites. Jilin-1 KF01, characterised by a notable ultra-wide swath width of 136 km, provides the user community with Very High Resolution (**VHR**) multispectral (**MS**) and panchromatic (**PAN**) imagery of the Earth’s surface.

The results of the assessments performed on the sample of **orthorectified bundle** products (KF01A mostly) procured from the data provider, **Head Aerospace**, between April and September 2021, are summarised in Table 2-1.

Table 2-1: Jilin-1 KF01: Assessment Area Results

Assessment Area	Results
KF01A / B Ground Sampling Distance (GSD) / Pixel Size @ Nadir: Panchromatic 0.75 m / 0.5 m Multispectral 3.0 m / 2.0 m.	
Geometric Calibration Quality	<p>1. Absolute Geolocation Accuracy</p> <p>The results of this assessment indicate the (average) absolute geolocation accuracy of orthorectified multispectral and panchromatic imagery is 12.94 m and 6.95 m CE90, respectively. Therefore, the minimum performance requirement specified by the operator as < 20.0 m CE90 [RD-7] has been met.</p> <p>2. Temporal Geolocation Accuracy</p> <p>The temporal geolocation accuracy could not be assessed due to the very small sample of suitable products procured.</p> <p>Note a minimum performance requirement has not been specified by the operator for this metric.</p> <p>3. Band Co-registration Accuracy</p> <p>The results of this assessment indicate the band co-registration accuracies of the multispectral band pairs (blue-green, green-red and red-near-infrared) is 0.22, 0.23 and 0.36 multispectral pixels CE90, respectively. The latter is associated with a small error budget (i.e. error associated with the method).</p> <p>The band co-registration accuracies of the multispectral-panchromatic band pairs are far lower, but this may be due to these bands being co-registered for pansharpened imagery only (pansharpened products available).</p>

	<p>Note a minimum performance requirement has not been specified by the operator for this metric.</p>
<p>Radiometric Calibration Quality</p>	<p>1. Absolute Radiometric Accuracy</p> <p>The results of this assessment indicate the data is poorly calibrated (absolute radiometric accuracy < 30 %) and the reason(s) for this is not clear at this time. However, as the latter appears to be prevalent with the other Jilin-1 missions assessed, it could be due to the calibration method used and so it is recommended the operator re-assesses their calibration method.</p> <p>Note a minimum performance requirement has not been specified by the operator for this metric.</p> <p>2. Temporal Radiometric Accuracy</p> <p>The temporal radiometric accuracy could not be assessed due to the very small sample of suitable products procured.</p> <p>Note a minimum performance requirement has not been specified by the operator for this metric.</p>
<p>Image Quality</p>	<p>1. Modulation Transfer Function</p> <p>This assessment could not be performed as the tool used could not precisely detect or define the edges of the chosen artificial modulation transfer function target (i.e. blurring is evident, poor sharpness indicates degradation of image quality). This may be because the modulation transfer function compensation correction had not been applied during processing, as indicated in the product metadata (this parameter is not sufficiently detailed in [RD-3]).</p> <p>Note a minimum performance requirement has been specified by the operator as > 0.16 (assumed at N_f).</p> <p>2. Signal-to-Noise Ratio</p> <p>The results of this assessment indicate the signal-to-noise ratio is good and well above the minimum performance requirement specified by the operator as > 100:1 (assumed to apply for all bands). However, this minimum performance requirement should be specified alongside reference top-of-atmosphere radiances as is commonly done so.</p> <p>3. Image Interpretability</p> <p>The results of this assessment indicate the interpretability of this imagery is reasonable (i.e. features or objects of interest, especially of those applicable to the NIIRS category of this sensor, can be interpreted) but there is room for improvement.</p>

Visual Inspections	The results of this assessments indicate there are no anomalies or artefacts present in the products procured.
---------------------------	--

3. EDAP QUALITY ASSESSMENT

3.1 EDAP Maturity Matrix

Table 3-1 Maturity Matrix for KF01

Product Information	Product Generation	Ancillary Information	Uncertainty Characterisation	Validation
Product Details	Sensor Calibration & Characterisation Pre-launch	Product Flags	Uncertainty Characterisation Method	Reference Data Representativeness
Product Availability & Accessibility	Sensor Calibration & Characterisation Post-launch 🔒	Ancillary Data	Uncertainty Sources Included 🔒	Reference Data Quality
Product Format 🔒	Additional Processing 🔒		Uncertainty Values Provided 🔒	Validation Method
User Documentation			Geolocation Uncertainty 🔒	Validation Results
Metrological Traceability Documentation				

Key
Not Assessed
Not Assessable
Basic
Intermediate
Good
Excellent

🔒 Information not public

3.1.1 Product Information

Product Details	
<i>Grade: Intermediate</i>	
<i>Justification: As there is some required and recommended information (included in product metadata, documentation, etc.) missing, especially for KF01B as the mission is relatively new and so the documentation has not been updated, the status of this section of the maturity matrix has been graded as “Intermediate”.</i>	
Product Name	<i>KF01A / B Bundle Standard Orthorectified</i>
Sensor Name	<i>KF01A / B (“Earth Scanner”)</i>
Sensor Type	<i>(Pushbroom) Optical (Visible and Near-Infrared): Blue: 450 – 510 nm Green: 510 – 580 nm Red: 630 – 690 nm Near-Infrared: 770 – 895 nm Panchromatic: 450 – 800 nm</i>
Mission Type	<i>Twin Satellites</i>
Mission Orbit	<i>KF01A: Sun-synchronous (482 km Altitude, 10:00 AM Descending Node Local) KF01B: Sun-synchronous (Altitude and Descending Node Local not known)</i>
Product Version Number	<i>(Not provided)</i>
Product ID	<p><i>JL1KF01A_PMS04_20200707180240_200027911_103_002_1_001_L3A</i></p> <p><i>Satellite Name (JL1KF01x: A or B), Detector Name and Number (PMS0x: 1 – 6), Imaging Time (YYYYMMDDHHMMSS (Beijing Local)), Mission Planning Number, Segment Number, Scene Number, Production Times, Product Level.</i></p> <p><i>Note the operator has confirmed for this sensor “The naming of PMS0x is for the tiling separation of each image (equivalent to scene size 136 / 6 ≈ 23 km), where East<-----> West PMS06 - PMS05 - PMS04 - PMS03 - PMS02 - PMS01.”</i></p> <p><u>Important note:</u> <i>The operator has confirmed the solar and viewing geometry angles given in the product metadata are applicable to the nadir only (i.e. not re-calculated for each PMS) and so any higher-level processing, where this information is deemed vital (e.g. bidirectional reflectance distribution function corrections and atmospheric corrections), would have errors introduced from using the metadata for the nadir when the tile is not or near the nadir tile. The latter needs to be made clear in the user documentation.</i></p>

Product Processing Level	<table border="1"> <tr> <td>L1</td> <td>Based on L0 product, sensor and radiometric correction products, this level product includes RCP files.</td> </tr> <tr> <td rowspan="3">L3</td> <td>A</td> <td>Based on L1 products, orthorectified products with its correspondent projection information.</td> </tr> <tr> <td>B</td> <td>Based on L3A products, it is reflective pre-orthorectified product with atmospheric correction.</td> </tr> <tr> <td>C</td> <td>Based on L3A product, it provides fusion product combining a high-resolution panchromatic image (PAN) with a low-resolution multispectral image (MS).</td> </tr> <tr> <td>L5</td> <td>Mosaiced image are orthorectified and color balanced products. Image framing is performed according to image GSD.</td> </tr> </table>	L1	Based on L0 product, sensor and radiometric correction products, this level product includes RCP files.	L3	A	Based on L1 products, orthorectified products with its correspondent projection information.	B	Based on L3A products, it is reflective pre-orthorectified product with atmospheric correction.	C	Based on L3A product, it provides fusion product combining a high-resolution panchromatic image (PAN) with a low-resolution multispectral image (MS).	L5	Mosaiced image are orthorectified and color balanced products. Image framing is performed according to image GSD.
	L1	Based on L0 product, sensor and radiometric correction products, this level product includes RCP files.										
L3	A	Based on L1 products, orthorectified products with its correspondent projection information.										
	B	Based on L3A products, it is reflective pre-orthorectified product with atmospheric correction.										
	C	Based on L3A product, it provides fusion product combining a high-resolution panchromatic image (PAN) with a low-resolution multispectral image (MS).										
L5	Mosaiced image are orthorectified and color balanced products. Image framing is performed according to image GSD.											
	<i>The products used for these assessments are those generated by Level 1 and Level 3A product processing levels (specification above taken from [RD-3]).</i>											
Measured Quantity Name	<i>Digital Numbers (12-bit scaled to 16-bit) / Spectral Radiance</i>											
Measured Quantity Units	<i>Unitless / W.sr⁻¹.m⁻².µm⁻¹</i>											
Stated Measurement Quality	<i>Radiometric Calibration Quality (Accuracy): Not Specified. Geometric Calibration Quality (Accuracy): CE90 < 12.0 m @ Nadir.</i>											
Spatial Resolution	<i>Very High Resolution</i> <i>Multispectral:</i> <i>KF01A 3.0 m GSD @ Nadir</i> <i>KF01B 2.0 m GSD @ Nadir</i> <i>Panchromatic:</i> <i>KF01A 0.75 m GSD @ Nadir</i> <i>KF01B 0.5 m GSD @ Nadir</i> <i>Full Swath Width @ Nadir: 136.0 km</i> <i>Scene Size @ Nadir 23 x 23 km</i>											
Spatial Coverage	<i>Global</i>											
Temporal Resolution	<i>Revisit < 4 Days for 1 Satellite, 2 Days for 2 Satellites (Latitude Dependent)</i>											
Temporal Coverage	<i>Mission Lifetime > x Years (Not provided)</i>											
Point of Contact	<i>contact@head-aerospace.fr</i>											
Product locator (DOI/URL)	<i>The sensor products are made available upon request (orders / tasks are placed with the data provider's imagery support team: contact@head-aerospace.fr) or through their online catalogue (https://headfinder.head-aerospace.eu/pub).</i>											
Conditions for access and use	<i>The standard license for imagery, adapted on a case-by-case basis (i.e. depending upon the needs of the user), is delivered to the customer by the Head Aerospace sales team (contact e-mail address provided above).</i>											
Limitations on public access	<i>No public access.</i>											
Product Abstract	<i>The product abstract, for all product types, is provided in [RD-3].</i>											

Availability & Accessibility	
<i>Grade: Intermediate</i>	
<i>Justification: The products and their content are compliant with many of the Findable, Accessible, Interoperable and Reusable (FAIR) Data Principles for scientific data management and stewardship [RD-6]. The data is available to users, at cost, through an easy-to-access commercial license.</i>	
Compliant with FAIR principles	<i>The products and their content are compliant, where applicable, with many of the Findable, Accessible, Interoperable and Reusable (FAIR) Data Principles for scientific data management and stewardship [RD-6]. It is recommended, however, to have the data be released with a clear and accessible data usage licence.</i>
Data Management Plan	<i>This is not shared by the data provider.</i>
Availability Status	<i>As mentioned previously, the products are made available upon request (orders / tasks are placed with the data provider's imagery support team: contact@head-aerospace.fr) or through their online catalogue (https://headfinder.head-aerospace.eu/pub).</i>

Product Format	
<i>Grade: Intermediate</i>	
<i>Justification: The product format and content, in which standard file formats and naming conventions are generally used, is only partially described in [RD-3]; product metadata file format and content is not fully described and product quality metadata file format and content, with valuable / useful data, is not described at all (this includes units and how the values for quality parameters are calculated / determined).</i>	
<i>It is recommended that existing documentation be updated in order to ensure the format and contents of all products are described fully, where applicable, for full understanding of the product. It is also recommended, for ease of use by the user, that timestamps (in product name and metadata) are not given in Beijing Local Time but in UTC.</i>	
<i>The data is not considered as analysis ready data (e.g. Committee for Earth Observing Satellites (CEOS) Analysis Ready Data, https://ceos.org/ard/).</i>	
Product File Format	<i>The product format ensures the following imagery and metadata files, adopting standard file formats i.e., includes the following:</i> <ul style="list-style-type: none"> •Product Image (.TIF) •Product Image Metadata (.XML) •Product Image Quality Metadata (.XML) •Product Browse Image Icon (.JPG) •Product Browse Image Icon Thumbnail (.JPG) <i>The product format applies to the product procured for these assessments (i.e. L3A) but deviations to this product format exist for products of a different type.</i>
Metadata Conventions	<i>Not implemented as optional (e.g. Geographic Information – Metadata ISO).</i>
Analysis Ready Data?	<i>No</i>

User Documentation		
<i>Grade: Basic</i>		
<i>Justification: The product user guides, provided upon request to the data provider, contain high-level information only (e.g. basic description of sensor, product type and processing level, and spectral information and instructions that allows users to convert data from digital numbers to top-of-atmosphere reflectance). The product user guide, or any other documentation made available, does not contain algorithm theoretical basis document-type information. Therefore, the status of this section of the maturity matrix has been graded as “Basic”.</i>		
Document	Reference	QA4ECV Compliant
Product User Guide (Chang Guang)	[RD-3]	No
Product User Guide (Head Aerospace)	[RD-4] Draft. Not yet made available.	No
Data Sheet	[RD-7]	No
Algorithm Theoretical Basis Document	Documentation not made available.	N/A

Metrological Traceability Documentation		
<i>Grade: Not assessable.</i>		
Document	Reference	
Traceability Chain / Uncertainty Tree Diagram Available	Document not made available.	

3.1.2 Product Generation

Sensor Calibration and Characterisation – Pre-Launch	
<i>Grade: Basic</i>	
<i>Justification: There is very basic information (i.e. stated values and not methodology used) provided on pre-launch radiometric calibration and characterisation, using the radiometric and spectral calibration test platform of Chang Guang Satellite Technology, only. As there is no information on pre-launch spectral or spatial calibration and characterisation activities, this section of the maturity matrix has been graded as ‘Basic’.</i>	
Summary	<i>This document provides high-level information on the radiometric calibration of all sensors within the Jilin-1 constellation. However, the document is not made available to users.</i>
References	[RD-5] Documentation not made available to users.

Sensor Calibration and Characterisation – Post-Launch	
<i>Grade: Basic</i>	
<i>Justification: There is very basic information (i.e. stated values and not methodology used) provided on post-launch radiometric calibration and characterisation, using primarily cross-calibration methods, only. As there is no information on post-launch spectral or spatial calibration and characterisation activities, this section of the maturity matrix has been graded as ‘Basic’.</i>	

Summary	<i>This document provides high-level information on the radiometric calibration of all sensors within the Jilin-1 constellation. However, the document is not made available to users.</i>
References	<i>[RD-5] Documentation not made available to users.</i>

Additional Processing	
<i>Grade: Basic</i>	
<i>Justification: There is no documentation on the processing steps carried out for orthorectification, apart from the brief mention of the use of the NASA Shuttle Radar Topographic Mission 90 m spatial resolution at equator SRTM90 DEM, and so this section of the maturity matrix has been graded as 'Basic'.</i>	
Summary	<i>Orthorectification</i>
References	-

3.1.3 Ancillary Information

Ancillary Data	
<i>Grade: Basic</i>	
<i>Justification: The key ancillary data required to define measurement data does not, importantly, include the following:</i>	
<ul style="list-style-type: none"> • <i>The viewing geometry given in the product metadata is only applicable to the tile(s) closest to the nadir, which means there will be a deviation / error in the true measurement values for tiles towards the edge of the swath.</i> • <i>The viewing geometry for non-nadir viewing is not accurately calculated or reported in the product metadata (e.g. viewing angle of the acquisition; the operator said the roll angle can be used as the viewing angle, however, this is not strictly true as the viewing angle needs to take into account the pitch angle (the latter is only true when the pitch angle equals zero)).</i> • <i>The uncertainties associated with the measurement data.</i> 	
<i>Therefore, this section of the maturity matrix has been graded as 'Basic'.</i>	
Description	<p><i>The product-specific ancillary data (e.g. nadir viewing and solar geometry angles, longitude, latitude, altitude), used to define measurements, can be found in product metadata and general ancillary data (e.g. in-band solar irradiance) can be found in the accompanying documentation (e.g. product guide, other documentation requested from the data provider). However, uncertainties have not been quantified, where applicable, for ancillary data.</i></p> <p><i>It is important to note that all viewing and solar geometry details included in the product metadata are only applicable to the PMS covering the nadir.</i></p>
Reference	-

Product Flags

<i>Grade: Not Assessable</i>	
<i>Justification: These products do not contain flags, in their conventional form, and so this section of the maturity matrix has been graded as 'Not Assessable'.</i>	
Description	<i>The products do not contain flags in the conventional form (e.g. bit settings) but they do contain quality information which can be used as flags (e.g. cloud content, product quality grade, etc.).</i>
Reference	-

3.1.4 Uncertainty Characterisation

Uncertainty Characterisation Method	
<i>Grade: Not Assessable</i>	
<i>Justification: The methods used to characterise the uncertainties associated with geometric and radiometric calibration quality are not included in the documentation made available to users, and so this section of the maturity matrix has been graded as 'Not Assessable'.</i>	
Description	<i>(See above)</i>
Reference	-

Uncertainty Sources Included	
<i>Grade: Basic</i>	
<i>Justification: There is <u>only</u> information / documentation concerning the sources of uncertainty related to the pre-launch radiometric calibration and characterisation of the sensor (the aforementioned radiometric calibration of Jilin-1 sensor document shared only with the EDAP team). Therefore, this section of the maturity matrix has been graded as 'Basic'.</i>	
Description	<i>(See above)</i>
Reference	-

Uncertainty Values Provided	
<i>Grade: Basic</i>	
<i>Justification: The documentation provides single uncertainty values that are used to characterise geometric performance per-product and for the mission as a whole only, and so this section of the maturity matrix has been graded as 'Basic'.</i>	
<i>It is recommended the operator provides uncertainty values used to characterise the radiometric performance (e.g. absolute radiometric accuracy) for the whole mission.</i>	
Description	<i>(See above)</i>
Reference	-

Geolocation Uncertainty	
<i>Grade: Intermediate</i>	
<i>Justification: A single geolocation uncertainty (i.e. geolocation accuracy) value, typically described as a circular error, is provided for the whole mission and a single geolocation uncertainty value is provided per product (found in the quality metadata file as <GeoPrecision> but this an assumption as the product guide does not document this parameter) and so this</i>	

section of the maturity matrix has been graded as 'Intermediate'. Note the calculation of the latter is not known.	
Description	The geolocation uncertainty associated with orthorectified data for this mission is < 20 m (applicable to full range of viewing angles), without ground control.
Reference	[RD-4]

3.1.5 Validation

It is important to note this section, relating to the 'Validation' column of the maturity matrix, is based on the results of the preliminary data quality assessments performed by the EDAP Optical team **only** (i.e. **independently** of any data quality assessments performed by the data provider and / or operator).

Reference Data Representativeness	
<i>Grade: Basic</i>	
<i>Justification: The representativeness of used reference data (sensor data from similar or 'gold' standard missions, in-situ data, ground control data), against which this sensor data is compared against, is good but the variety of reference data is small compared with the reference data available. Therefore, this section of the maturity matrix has been graded as 'Basic'.</i>	
Summary	(See above)
References	-

Reference Data Quality and Suitability	
<i>Grade: Intermediate</i>	
<i>Justification: The reference data quality and suitability used by EDAP comes with a single uncertainty value for the entire sensor mission and so this section of the maturity matrix has been graded as 'Intermediate'</i>	
Summary	<p><i>The data used as reference for some of the radiometric calibration quality assessments include in-situ reference data from the well-established and documented RadCalNet.</i></p> <p><i>The data used as reference for the geometric calibration quality assessments include orthorectified panchromatic imagery from SPOT-5, which is validated by CNES as 2.5 m RMSE absolute accuracy, and ground control points, derived during a field survey with the Differential Global Positioning System, with an absolute accuracy as 0.10 m RMSE.</i></p> <p><i>The data used as reference for the image quality assessments include orthorectified multispectral imagery from Pléiades.</i></p>
References	[RD-8]

Validation Method
<i>Grade: Intermediate</i>

<i>Justification: The validation methods used, despite being well-documented and used by the scientific community, produce simple uncertainty values (e.g. from a statistical distribution of results) and so this section of the maturity matrix has been graded as 'Intermediate'.</i>	
Summary	<i>The validation methods used to assess image quality, geometric calibration and radiometric calibration quality are all well-documented and used by the scientific community.</i>
References	<i>[RD-8], [RD-10]</i>

Validation Results	
<i>Grade: Intermediate</i>	
<i>Justification: The validation results, from validation assessment performed independently of those performed by the operator, show good agreement between satellite sensor and reference measurements (and within uncertainties), with the exception for the validation results of radiometric calibration quality and so this section of the maturity matrix has been graded as 'Intermediate'.</i>	
Summary	<i>The validation results of all assessments are summarised in Section 0.</i>
References	<i>See Section 4 and 5.</i>

4. DETAILED Jilin-1 KF01 QUALITY ASSESSMENTS

4.1 Objectives

The objective of this work is to assess all core aspects of sensor data quality (geometric calibration, radiometric calibration, image quality) against sensor and product performance requirements or specifications, using the sample of sensor products procured.

4.2 Geometric Calibration Quality

This section describes the assessment of geometric calibration quality of sensor products, detailed in Table 4-1, in terms of **absolute geolocation accuracy**, **temporal geolocation accuracy** and **band co-registration accuracy**.

Table 4-1: Geometric Calibration Quality Assessment Product Sample

Location	Product	Product Name (JL1KF01)	Roll Angle / Sensor Viewing Angle (°)
La Crau (France)	1	A_PMS04_20200707180240_200027911_103_0021_001_L3A	-4.86
	2	B_PMS05_20210905181026_200060331_103_0001_001 ¹ _L3A	-0.00
	3	B_PMS05_20210905181026_200060331_103_0002_001_L3A	-0.00
Salon-de-Provence (France)	4	A_PMS01_20210615174508_200052889_103_0002_001_L3A	-12.79
	5	A_PMS05_20210527175657_200051097_102_0001_001_L3A	0.00

Please note the following assessments must take into consideration the satellite and tile / detector number.

4.2.1 Absolute Geolocation Accuracy

4.2.1.1 Description and Method I (Panchromatic)

The absolute geolocation (planimetric) accuracy of orthorectified panchromatic imagery is assessed using a method that directly determines the difference between the actual and apparent location of a set of ground control points (**GCPs**) that have been defined by the Differential Global Positioning System (**DGPS**) during a field survey.

This assessment was performed on the following product(s):

¹ This parameter indicates the scene number, the number for scene cataloguing of a section of continuously imaged strip or segment of data (defined by the previous parameter, '103'). Note product 2 and 3 are subsequent scenes from the same segment of data.

La Crau (France)

Product 1, Product 2, Product 3

The orthorectified imagery included in these three products have been used to determine the absolute geolocation accuracy of *relatively low and homogenous topography*. Note the topography of La Crau does not exceed 190 m above the ellipsoid.

The orthorectified imagery required to determine the absolute geolocation accuracy of *relatively high and inhomogeneous topography* has, unfortunately, not been procured due to tasking priorities by the operator.

The minimum performance requirement for the absolute geolocation accuracy of this sensor has been specified as < 20 m CE90 [RD-4] (assumed applicable to $\pm 45^\circ$ viewing angles and for both sensors). Note it is common for the absolute geolocation accuracy to be described as a circular error at a specified percentile (e.g. CE90 means that a minimum of 90 % of the points measured have an error that is less than the stated CE90 value).

4.2.1.2 Results I

The results of this assessment are detailed in Table 4-2 and Figure 4-1 - Figure 4-3.

Table 4-2 La Crau (France) Panchromatic (Planimetric) Absolute Geolocation Accuracy Assessment Results

Parameter	Product 1	Product 2	Product 3
GCP Sample #	12	9	15
Mean Easting Error (m)	-2.29	-2.81	0.80
Mean Northing Error (m)	1.77	2.99	-1.60
Easting Error Standard Deviation (m)	2.62	2.05	2.92
Northing Error Standard Deviation (m)	2.85	2.92	2.86
Easting Root Mean Square Error (m)	2.90	3.48	3.03
Northing Root Mean Square Error (m)	3.36	4.18	3.28
Root Mean Square Error (m)	4.44	5.44	4.46
CE90 (m)	6.71	7.31	6.84

The results of this assessment indicate the minimum performance requirement has been met (i.e. independent of the satellite or detector); the (average) absolute geolocation accuracy of orthorectified panchromatic imagery over La Crau is 4.76 m RMSE and 6.95 m CE90, degraded only slightly by the observed bias (mean error, systematic error contribution) and the observed precision (standard deviation, random error contribution) in both directions.

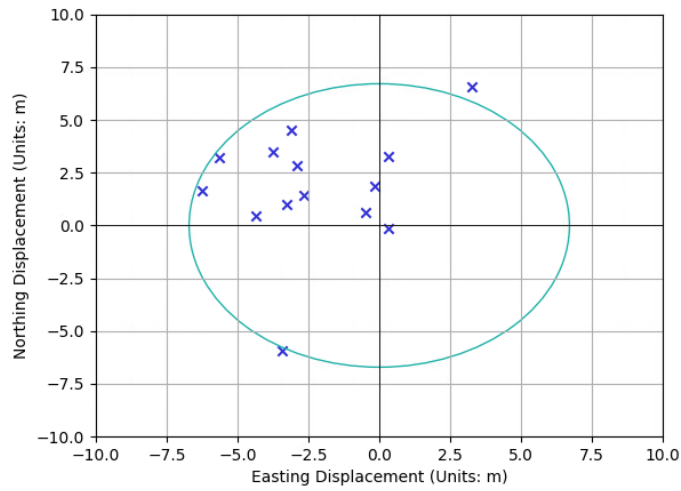


Figure 4-1 Product 1 Panchromatic Absolute Geolocation Accuracy (x GCP, - CE90).

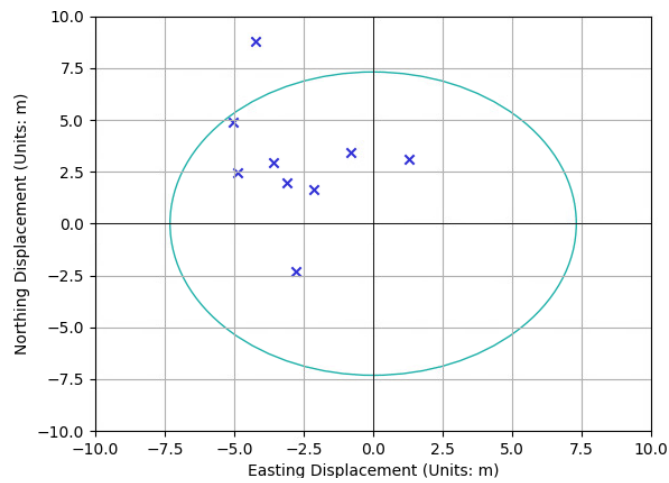


Figure 4-2 Product 2 Panchromatic Absolute Geolocation Accuracy (x GCP, - CE90).

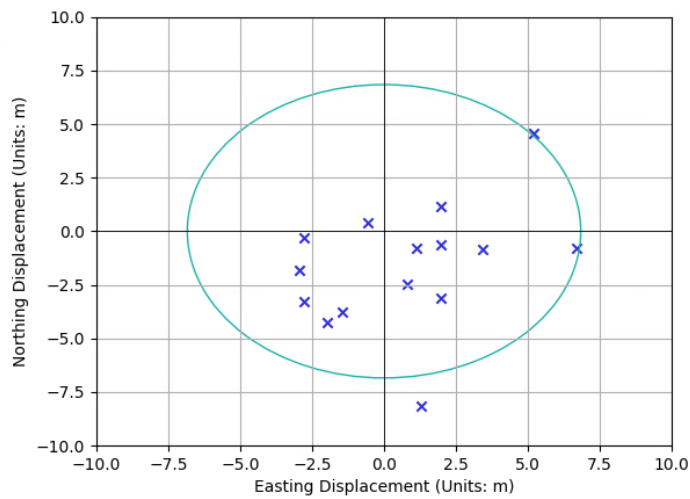


Figure 4-3 Product 3 Panchromatic Absolute Geolocation Accuracy (x GCP, - CE90).

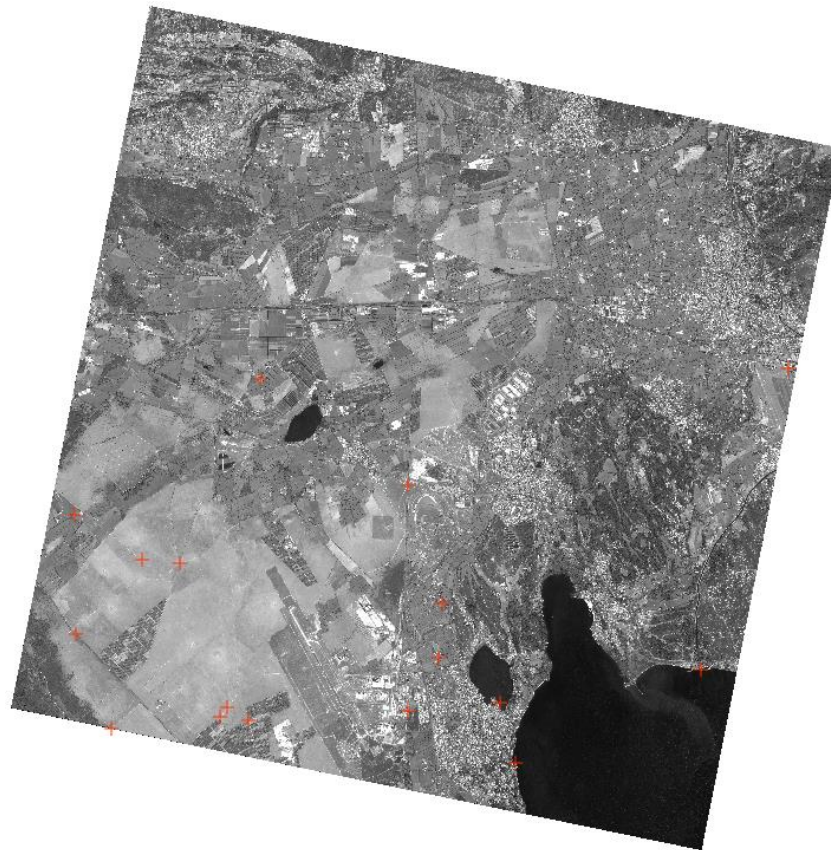


Figure 4-4 The number, density and distribution of GCPs (+) used to determine the absolute geolocation accuracy of orthorectified panchromatic imagery in Product 1 (left).

4.2.1.3 Description and Method and II (Multispectral)

The absolute planimetric geolocation accuracy of the sensor's multispectral imagery cannot be assessed using the same method adopted for the panchromatic imagery due to a lower spatial resolution (i.e. control points cannot be accurately identified). Therefore, the method used instead is one that involves the use of an image-matching tool (based on a zero mean normalised cross-correlation algorithm, validated sub-pixel / 0.2 m accuracy), provided by the CNES MEDICIS / QPEC tool [RD-12], between the sensor's multispectral imagery and (actual) multispectral imagery from a similar sensor that has been validated for use as reference.

This assessment was performed on the following product(s):

Salon-de-Provence (France)

Product 4 and **5** (red band)

Reference Product SPOT 5 20121008T093232 (Panchromatic band)

The reference imagery used for this assessment was from SPOT 5. It was delivered by CNES as free from systematic and non-systematic errors (i.e. due to terrain relief), and the absolute accuracy validated to be within 2.5 m (RMSE) [RD-15]; the main contributor to this slightly degraded accuracy was not the precision but actually the bias, which appeared

to be systematic, of about 1.5 m. This information is of importance when using this reference imagery.

4.2.1.4 Results II

The results of this assessment indicate the minimum performance requirement (i.e. independent of the satellite or detector) has been met; the (average) absolute geolocation accuracy of the orthorectified multispectral imagery over Salon-de-Provence is 8.47 m RMSE and 12.94 m CE90 (detailed in Table 4-3 and Figure 4-5), degraded only slightly by the observed bias (mean error, systematic error contribution) and the observed precision (standard deviation, random error contribution) in both directions.

Note image matching is performed at a specified confidence level (e.g. if the confidence level is specified as 95 % then the image matching results (i.e. geolocation accuracy) will be based on pixels that have been matched with 95% confidence / certainty).

Table 4-3 Multispectral Absolute Geolocation Accuracy Assessment Results (KF01 and SPOT 5 Image Matching CL95%)

Parameter	Product 4	Product 5
Matched Pixels #	54	280
Mean Easting Error (m)	2.78	-1.33
Mean Northing Error (m)	-4.51	-3.88
Easting Error Standard Deviation (m)	5.87	6.04
Northing Error Standard Deviation (m)	3.59	3.86
Easting Root Mean Square Error (m)	6.50	6.18
Northing Root Mean Square Error (m)	5.76	5.47
Root Mean Square Error (m)	8.68	8.26
CE90 (m)	13.18	12.70

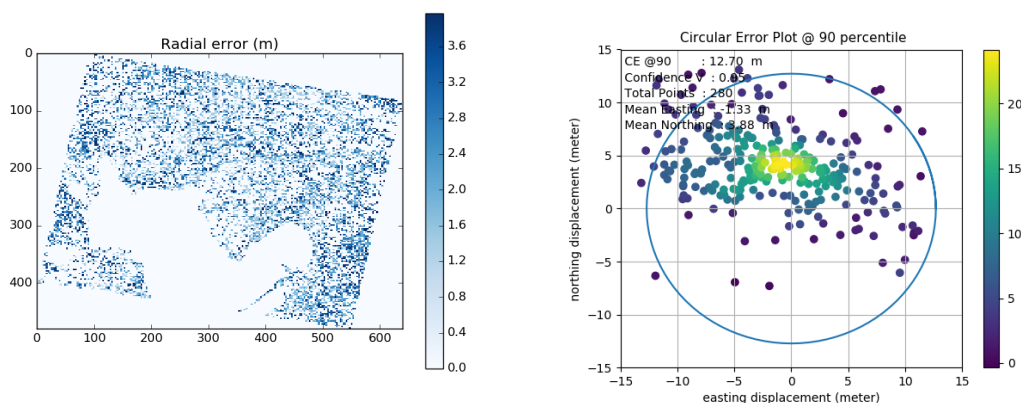


Figure 4-5 Image matching tool results for product 4 and reference SPOT 5 imagery (radial error per matched pixel (left), directional and circular error per matched pixel (right)).

Note it is also important to consider the limitations of using intensity-based image matching algorithms as it includes errors originating from differences in viewing geometries, solar

geometries (e.g. shadow), ground conditions (wet or dry ground), atmospheric conditions and temporal baseline between compared imagery.

4.2.2 Temporal Geolocation Accuracy

The temporal geolocation accuracy could not be assessed for this sensor due to the very small sample of suitable products procured.

4.2.3 Band Co-registration Accuracy

4.2.3.1 Description and Method

The multispectral and panchromatic band co-registration accuracy been assessed using the aforementioned image matching tool, where it was applied to the imagery of each pair of adjacent bands (e.g. blue (**band 1**) and green (**band 2**), green and red (**band 3**), red and near-infrared (**band 4**), and near-infrared and panchromatic (**band 5**)).

This assessment was performed on the following products:

Product 1 and 3

Note there is no minimum performance requirement specified by the operator for band co-registration accuracy.

4.2.3.2 Results

The results of this assessment, detailed in Table 4-4 and Table 4-5, indicate the following band co-registration accuracies (averaged for the two products assessed):

- **Multispectral Band Co-registration**
 - **Band1_2 CE@90 < 0.870 m (0.44 MS Pixels)**
 - **Band2_3 CE@90 < 0.990 m (0.50 MS Pixels)**
 - **Band3_4 CE@90 < 1.540 m (0.77 MS Pixels)**
- **Multispectral-Panchromatic Band Co-registration**
 - **Band4_5 CE@90 < 10.006 m (5.00 MS Pixels)**

(Prior to starting the assessment, the pixel size of the panchromatic imagery is downsampled, using a cubic resampling kernel, to match that of the multispectral imagery.)

Table 4-4 Product 1: La Crau: Multispectral and Panchromatic Band Co-registration Accuracy (Image Matching Confidence Level @ 99 %). Units: Multispectral Pixels.

	Multispectral				Multispectral - Panchromatic	
	Band Pair: 1_2	Band Pair: 2_3	Band Pair: 3_4	Band Pair: 4_1	Band Pair: 4_5	Band Pair: 5_1
	Product 1					
# Matched Pixel Total	4754	3953	267	72	50	525
Mean Easting Error (px)	-0.037	0.033	0.008	0.006	-0.219	-1.037

Mean Northing Error (px)	-0.026	0.046	-0.017	-0.056	0.011	0.667
Easting Error Standard Deviation (px)	0.119	0.134	0.206	0.335	1.270	2.155
Northing Error Standard Deviation (px)	0.121	0.144	0.250	0.304	0.988	1.670
Easting Root Mean Square Error (px)	0.125	0.138	0.206	0.335	1.288	2.391
Northing Root Mean Square Error (px)	0.124	0.152	0.251	0.309	0.988	1.798
Root Mean Square Error (px)	0.176	0.205	0.325	0.456	1.623	2.991
CE90 (m)	0.850	0.990	1.540	2.030	10.006	12.980

Table 4-5 Product 3: La Crau: Multispectral and Panchromatic Band Co-registration Accuracy (Image Matching Confidence Level @ 99 %). Units: Multispectral Pixels.

	Multispectral				Multispectral - Panchromatic	
	Band Pair: 1_2	Band Pair: 2_3	Band Pair: 3_4	Band Pair: 4_1	Band Pair: 4_5	Band Pair: 5_1
Product 3						
# Matched Pixel Total	3496	7069	1797	442	180	90
Mean Easting Error (px)	-0.044	-0.001	0.018	0.009	1.039	0.891
Mean Northing Error (px)	0.011	0.039	0.003	-0.082	0.402	-0.146
Easting Error Standard Deviation (px)	0.184	0.179	0.209	0.406	1.579	2.231
Northing Error Standard Deviation (px)	0.191	0.183	0.225	0.492	1.448	1.570
Easting Root Mean Square Error (px)	0.189	0.179	0.209	0.407	1.891	2.403
Northing Root Mean Square Error (px)	0.192	0.187	0.225	0.500	1.503	1.577
Root Mean Square Error (px)	0.270	0.259	0.307	0.644	2.416	2.874
CE90 (m)	0.870	0.840	1.020	2.120	7.930	9.010

The results of the band co-registration accuracy assessment indicate the multispectral bands are reasonably well co-registered (commonly aiming for sub-pixel, usually CE90 < 0.3 MS pixels (e.g. Vision-1, Sentinel-2)). The multispectral-panchromatic bands, however, appear to be poorly co-registered but this is mostly likely due to the products assessed being bundle and not pansharpened products (extra corrections would ensure multispectral-panchromatic band co-registration accuracy is high).

In addition to the above, the error budget is computed (in this case, only for the multispectral bands), and it is based on the rule that per pixel displacement errors are transitive across all band pairs - by summing the displacement for all band pairs (e.g. (1, 2), (2, 3), (3, 4), the result is in the same order of displacement for the band pair (1, 4), as shown in the equation below:

$$D_{1,4} \cong D_{1,2} + D_{2,3} + D_{3,4}$$

Where $D_{1,4}$ stands for displacement between band 1 and 4 (calculated for the easting and northing direction).

By comparing this estimate $D_{1,4}$ against the true value ($D_{4,1}$) obtained with image matching, the error budget of the method is computed (i.e. error budget = $D_{1,4} + D_{4,1}$ or $D_{1,4} - D_{4,1}$);

the (average) error budget in the easting and northing directions is 0.01 and 0.03 MS pixels, respectively. These small error budgets indicate the results are reliable.

JL1KF01A_b1_b2_C=0.99

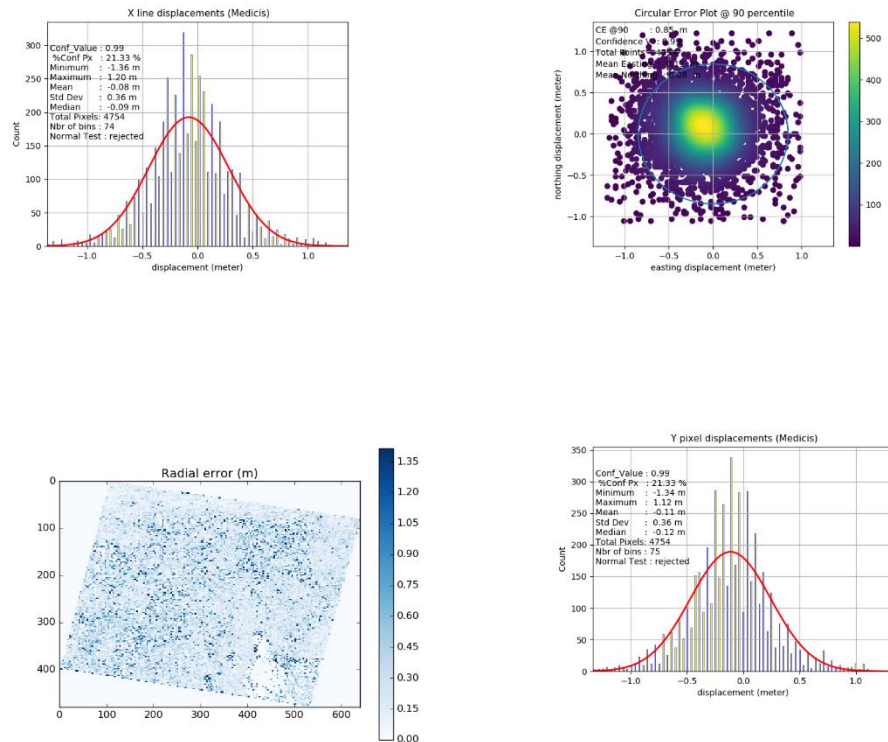


Figure 4-6 The band co-registration assessment outputs of band 1_2 from Product 1.

Note the product quality metadata files contains information on what appears to be band co-registration accuracy metrics, using a different multispectral band (only) configuration (e.g. band 1_2, band 1_3, where band 1 is the reference band). However, comparisons cannot be made to the results detailed in the tables above, where applicable, as it is not completely clear how these metrics have been calculated or what their units are.

Note the two products assessed here are from two different satellites so no clear relationship can be made or commented on (i.e. more products for each satellite would need to be assessed).

4.3 Radiometric Calibration Quality

This section describes the assessment of radiometric calibration quality of sensor products, detailed in Table 4-6, in terms of the **absolute** and **temporal radiometric accuracy**.

Table 4-6: Radiometric Calibration Quality Assessment Product Sample

Location	Product	Product Name (JL1KF01)
La Crau (France)	1	A_PMS04_20200707180240_200027911_103_0021_001_L3A
	2	(No RadCalNet data available)
	3	(No RadCalNet data available)
Gobabeb (Namibia)	6	A_PMS01_20210208163646_200040344_102_0011_001_L3A
	7	A_PMS06_20210527164019_200051099_103_0001_001_L3A
	8	A_PMS06_20210622163841_200053495_103_0001_001_L3A

The radiometric calibration, or correction, of sensor data sees to the successful conversion of raw data (i.e. digital numbers) to spectral radiance or reflectance, using coefficients (e.g. physical bias, physical gain, solar spectral irradiance constants) derived pre-flight in laboratory conditions. This is important as it improves the interpretability and quality of the sensor data (and is particularly important when comparing multiple sensor datasets over a period of time, which is commonly performed by the scientific community).

The digital number (DN) to spectral radiance (L) conversion of sensor data, per band (b) is enabled by the following:

$$L_b = (DN_b * GAIN_b) + BIAS_b$$

The spectral radiance (L_b) to top-of-atmosphere reflectance (ρ_b), per band (b) is enabled by the following:

$$\rho_b = \frac{\pi * L_b * d^2}{E_{0b} * \sin(\theta_s)}$$

Where:

E_{0b} is solar spectral irradiance at the sensor for band b (units: $Wm^{-2}\mu m^{-1}$).

θ_s is solar elevation angle at the time / location of acquisition (units: degrees).

d^2 is Sun-Earth distance at the time of acquisition (units: astronomical units).

Note conversion formulae and coefficients mentioned above can be found in the product user guide, the product metadata and online.

4.3.1 Absolute Radiometric Accuracy

4.3.1.1 Description and Method

The method used to determine the absolute radiometric calibration accuracy of the sensor's bands is based on comparing the top-of-atmosphere (TOA) reflectance values derived from the sensor's acquisitions of the chosen RadCalNet calibration sites with the TOA reflectance values derived from the RadCalNet calibration sites (i.e. reference top-of-atmosphere reflectance values).

The RadCalNet calibration sites, operated by the CEOS Working Group for Calibration and Validation (**WGCV**) Infrared and Visible Optical Sensors (**IVOS**), provides the user community with the following:

- TOA reflectance values, derived from both in-situ surface and atmosphere measurements (e.g. surface pressure, columnar water vapour, columnar ozone, aerosol optical depth, etc.) that are **SI-traceable**, at:
 - 30-minute intervals between 09:00 and 15:00 local standard time (cloud-free data only), and 10 nm spectral sample intervals between 400 nm and 1000 nm.

Note the RadCalNet TOA reflectance values are representative of nadir viewing observations only, so comparison to sensor top-of-atmosphere reflectance values should be used with caution - when the sensor viewing zenith angle deviates significantly from nadir, both atmospheric and surface non-Lambertian behaviour can lead to significant deviation from at-nadir simulated signal. The correction for the latter (i.e. off-nadir viewing angle effects), as well as illumination (solar) angle effects, can be done using bi-directional reflectance modelling.

The products used to assess the absolute radiometric calibration accuracy, by temporal and spectral simulation with RadCalNet data, are the following:

Product 1, 6, 7 and 8 (Jilin-1 KF01A only)

These products provide acquisitions of the chosen RadCalNet calibration sites, La Crau (see Table 4-7) and Gobabeb (see Table 4-8).

Table 4-7 : RadCalNet La Crau Calibration Site Description

Parameter	Description
Geographic Location	Latitude: 43.558889, Longitude: 4.864167, Altitude: 20 m
Characteristics	The RadCalNet top-of-atmosphere reflectance spectra are representative of a disk of 30 m radius.

Table 4-8 : RadCalNet Gobabeb Calibration Site Description

Parameter	Description
Geographic Location	Latitude: -23.6002, Longitude: 15.1196, Altitude: 510 m
Characteristics	The RadCalNet top-of-atmosphere reflectance spectra are representative of a disk of 30 m radius.

The determined absolute radiometric accuracy cannot be evaluated against a minimum performance requirement as it has not been specified by the operator. Instead, this will be evaluated against what is generally considered very good, based on similar “gold standard” sensors such as Sentinel-2 and Landsat 8, which is approximately < 5 % for all bands [RD-17, RD-18].

4.3.1.2 Results

The results of this assessment, performed only for the multispectral bands, are detailed in Table 4-10 and Table 4-11.

Table 4-9 KF01 Sensor Observation Conditions (Solar and Viewing Geometries)

Product	Roll Angle / Sensor Viewing Angle (°)	Sensor Azimuth Angle (°)	Solar Elevation Angle (°)	Solar Azimuth Angle (°)	Water Vapour (g/cm)	AOD (m)
1 (PMS04)	-4.86	158.42	60.30	127.11	1.21	0.096
6 (PMS01)	4.63	170.646	52.28	83.79	4.87	0.066
7 (PMS06)	10.0	261.589	34.22	39.10	2.81	0.080
8 (PMS06)	8.69	260.45	31.61	38.93	2.89	0.012

Table 4-10 KF01A and Simulated KF01A (RadCalNet) TOA Reflectances

Product	Origin	ρ TOA Reflectance				
		Blue	Green	Red	NIR	PAN
1	Sensor	0.1148331	0.1105633	0.1263231	0.1833919	0.1444968
	RadCalNet	0.1355185	0.1413993	0.1745266	0.2501611	0.1789603
6	Sensor	0.1844921	0.2099050	0.2894801	0.3045590	0.2565548
	RadCalNet	0.1864759	0.2136646	0.2946928	0.3096642	0.2691237
7	Sensor	0.1610941	0.1613520	0.2421226	0.2336510	0.2193144
	RadCalNet	0.2010678	0.2290832	0.3098071	0.3263294	0.2836148
8	Sensor	0.1626412	0.1557946	0.2360421	0.2179514	0.1344659
	RadCalNet	0.1852429	0.1967505	0.2481246	0.2549586	0.2299238

Note the sensor TOA reflectances detailed in the table above have not had directional reflectance corrections applied, especially as the true viewing angles are not available.

The difference, expressed as a percentage, between Jilin-1 KF01A TOA reflectances ($\rho_b work$) and simulated Jilin-1 KF01A TOA reflectances ($\rho_b simulated$) is calculated as follows:

$$\rho_b = ((\rho_b simulated - \rho_b work) / (\rho_b simulated)) * 100$$

Table 4-11: Comparison between Jilin-1 KF01 and Simulated Jilin-1 KF01 RadCalNet TOA Reflectances

Product	ρ TOA Reflectance Difference (%)				
	Blue	Green	Red	NIR	PAN
1	15.26	21.81	27.62	26.70	19.26
6	1.06	1.76	1.77	1.65	4.67
7	19.88	29.56	21.85	28.40	22.67
8	12.20	20.81	4.87	14.51	41.52

The results of this assessment suggest that the data are poorly calibrated as the absolute radiometric accuracy is generally low and unstable. The cause(s) of the latter is not yet

clear, especially as the products assessed have viewing and solar geometries (and atmospheric conditions) within normal or ideal limits, but it may be due to the radiometric calibration method used by the operator² – all satellites in the Jilin-1 constellation are cross-calibrated with MODIS (MODIS bottom-of-atmosphere (BOA) reflectances propagated to TOA reflectances, using the 6SV radiative transfer model, for acquisitions over China and Africa only). Therefore, it is recommended that the operator re-assess their calibration method.

4.3.2 Temporal Radiometric Accuracy

The temporal radiometric accuracy is determined by producing a time-series of mean TOA reflectance, calculated for a defined area of interest, against the number of days since launch. However, this assessment could not be performed with the products procured (there are only two products of a suitable site (e.g. Libya-4, Product 9 and 10), from two different detectors of the same satellite, sensed only a few days apart).

4.4 Image Quality

The quality of imagery produced by a spaceborne optical imagery system / sensor is characterised by a complex relationship between the spatial sampling period / frequency, impulse response (also known as the point spread function) of the aforementioned system, radiometric noise, and possible on-ground digital post-processing for deblurring and denoising [RD-14]. It is the combination of these elements that define the quality and the amount of measurement – or more generally information – that can be extracted from the imaging system [RD-14].

This section describes the assessment of image quality on the supplied sensor products, detailed in Table 4-12, in terms of **Signal-to-Noise Ratio (SNR)**, **Modulation Transfer Function (MTF)** and **Image Interpretability**.

Table 4-12 Image Quality Assessment Product Sample

Location	Product	Product Name (JL1KF01)
La Crau (France)	1	A_PMS04_20200707180240_200027911_103_0021_001_L3A
	12	B_PMS05_20210905181026_200060331_103_0002_001_L1
	14	B_PMS05_20210905181026_200060331_103_0001_001_L3A
Gobabeb (Namibia)	6	A_PMS01_20210208163646_200040344_102_0011_001_L3A
	7	A_PMS06_20210527164019_200051099_103_0001_001_L3A
	8	A_PMS06_20210622163841_200053495_103_0001_001_L3A
Libya-4 (Libya)	9	A_PMS01_20210405162523_200046230_101_0001_001_L3A
	10	A_PMS04_20210401163212_200045798_101_0002_001_L3A

² When the relative difference between cross-calibration gain coefficients and ground calibration gain coefficients is greater than 10%, the cross-calibration coefficients will replace the ground calibration coefficient [RD-5].

Salon-de-Provence (France)	11	A_PMS05_20210527175657_200051097_102_0001_001_L3A
	13	A_PMS05_20210527175657_200051097_102_0001_001_L1

4.4.1 Signal-to-Noise Ratio

4.4.1.1 Description and Method

The SNR is used to quantify the performance of a sensor in response to a particular exposure; it quantifies the ratio of the sensor's output signal to the noise present in the output signal and can be expressed by the following:

$$SNR = \frac{\mu}{\sigma}$$

Where μ is the mean signal and σ is the standard deviation of the signal.

This assessment was performed on the following products:

Libya-4 (Libya, Africa)

Product 9 and 10

This bright desert site is a CEOS Pseudo-invariant Calibration Site (**PICS**), which has been chosen for this particular assessment because it is well known to exhibit reasonable spatial, spectral, and temporal uniformity and has minimal cloud cover. Note the presence of sand dunes in this site does not satisfy the criterion of flat terrain but the method described below accounts for this.

The method proposed for this assessment allows for the estimation of (spatial) SNR, based on the aforementioned equation and the following assumption:

- The mean signal is defined as the spatial average of a group of pixels observing a spatially varying scene and the noise is defined as the standard deviation of this signal for the same group of pixels.

The method, modified since it was initially proposed in [RD-11], is performed for each spectral band, whose imagery has been converted from digital numbers to radiance, in the following way:

1. Compute the local statistics of a small (5 x 5 pixels) sliding window applied to the imagery being assessed. Select only the "best" small windows for the following steps.
 - a. The selection of small windows ensures that increased site uniformity is generally maintained (if not, where spatially high frequencies exist (e.g. sharp transitions seen as dune summits, dedicated image processing is applied in order to detect this and filter (e.g. Sobel Filter)).
2. Compute the statistical distribution (histogram), between the **minimum** and **maximum radiance**, of the selected "best" small windows (statistics of 5 x 5 pixel windows) – the signal is defined as the peak (i.e. mean radiance) of this statistical distribution and the noise is defined as the standard deviation of this statistical distribution about the mean.

3. Estimate SNR(s).

Please note that SNR is an important image quality indicator - high SNRs are required in order to control uncertainties in radiometric measurements, especially multispectral bands, as much as possible.

4.4.1.2 Results

The results of this assessment are detailed in Table 2-1 and Figure 4-7 - Figure 4-9.

Table 4-13 Jilin-1 KF01 SNR Assessment Results

Band	Product 9		Product 10	
	Mean Radiance W.m ⁻² .str ⁻¹	SNR	Mean Radiance W.m ⁻² .str ⁻¹	SNR
Blue	114.07	307.89	104.07	252.27
Green	120.52	378.00	106.06	251.79
Red	159.02	326.92	144.88	221.25
NIR	107.41	324.19	97.70	238.89
PAN	166.34	476.25	152.16	338.37

The results of this assessment indicate strange values for both products (i.e. for all bands, the estimated SNR is much higher than one would expect, even for an optimum-performing sensor), but less so for product 10, but this may be due to the presence of cloud / cloud shadow (as is the case for product 9) or other quality factors (product quality grade for product 10 is B).

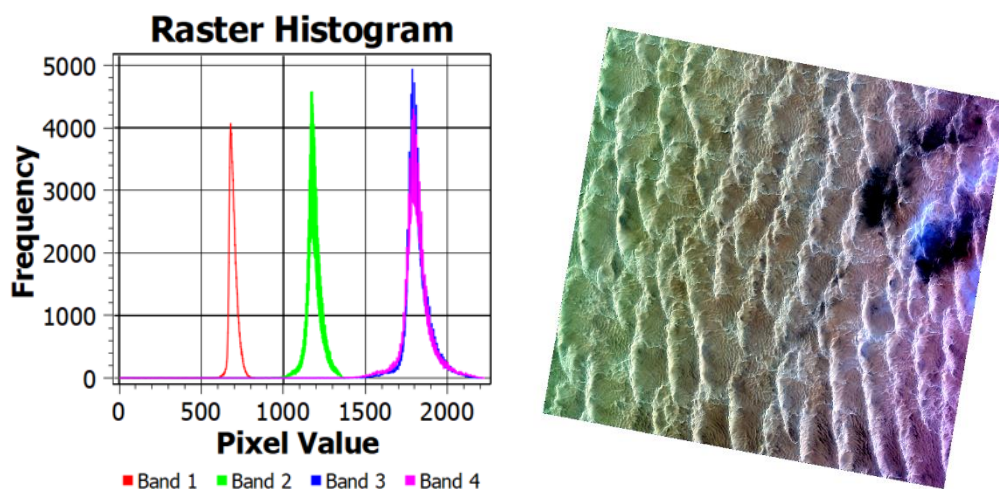


Figure 4-7 Histogram (left) and RGB (right) of multispectral image from Product 9 (note cloud and cloud shadow impact the default histogram stretch).

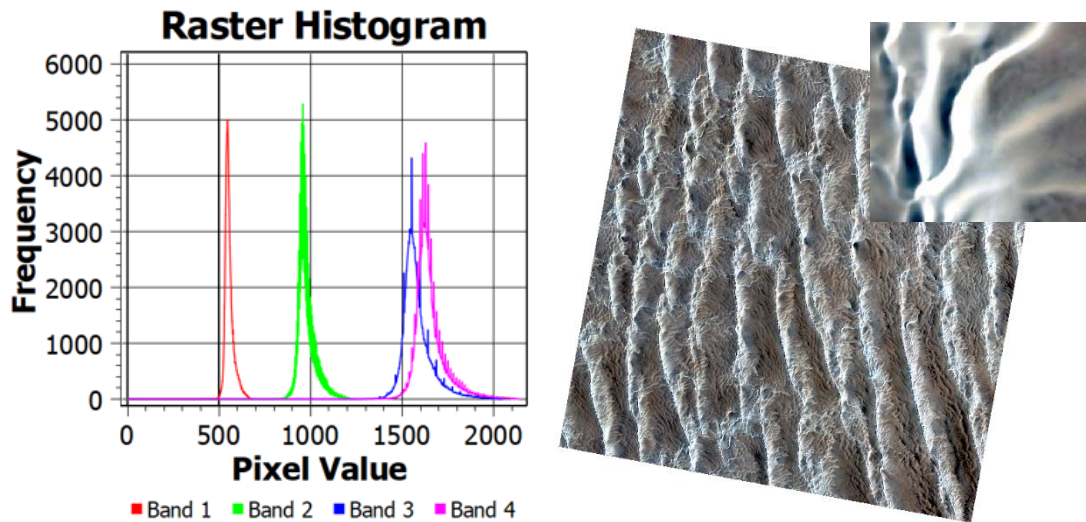
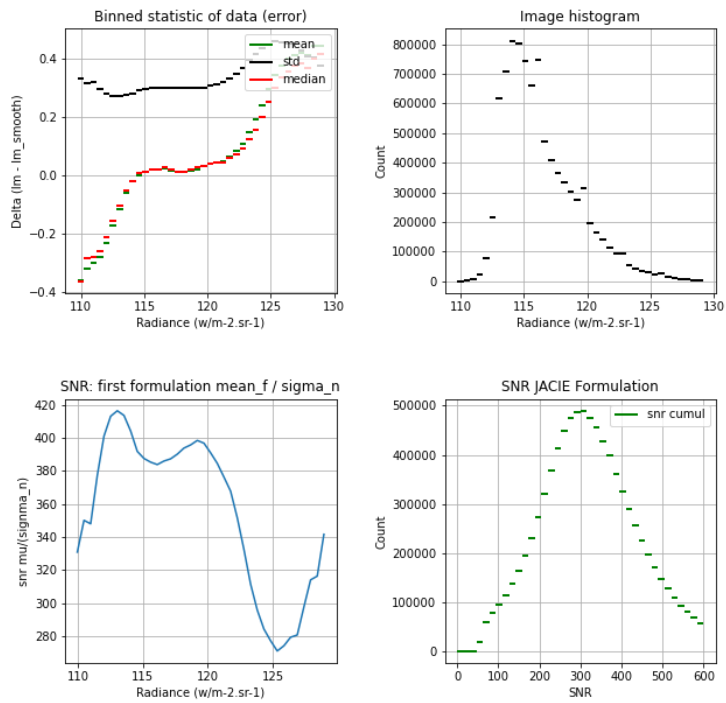
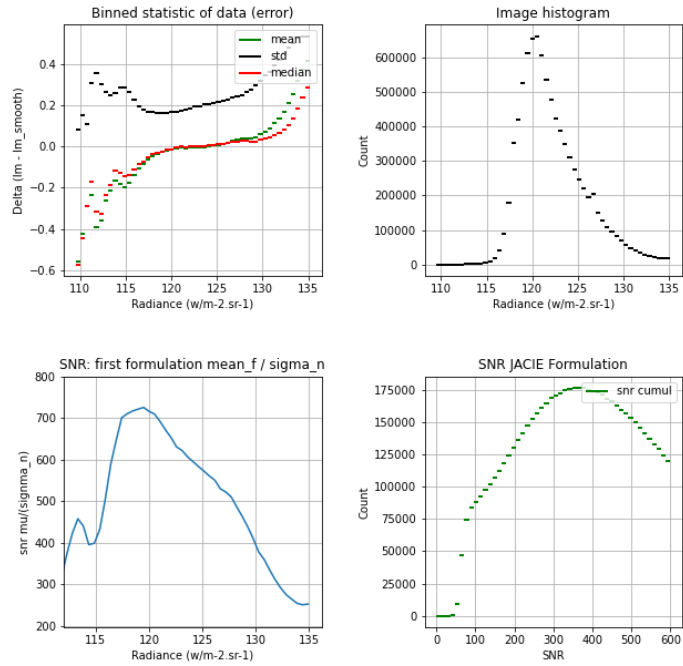


Figure 4-8 Histogram (left) and RGB (right) of multispectral image from Product 10.

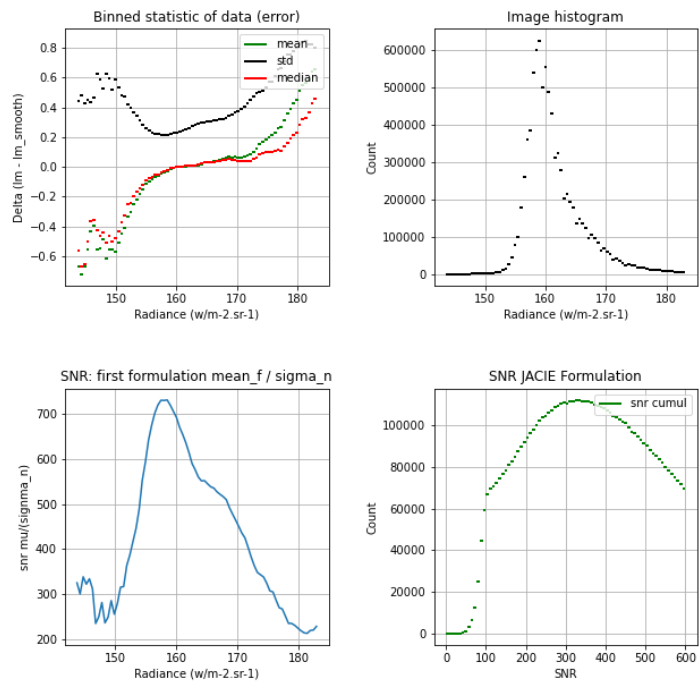
Band 1



Band 2



Band 3



Band 4

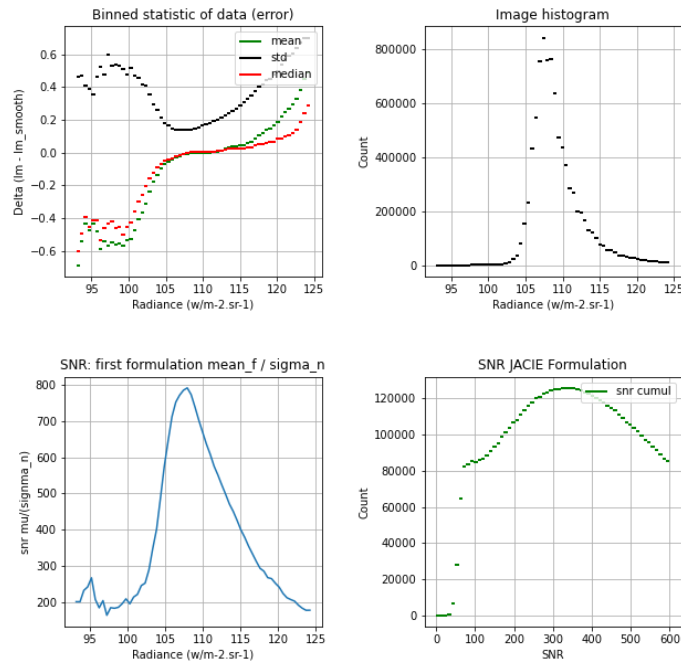


Figure 4-9 The SNR results for each band of Product 9.

The minimum performance requirement specified by the operator as >100:1 [RD-13] is not accompanied by reference radiances for each band and so the results of this assessment cannot be directly evaluated against this.

4.4.2 Modulation Transfer Function

4.4.2.1 Description and Method

The MTF importantly describes the response of the imaging sensor as a function of spatial frequency and so is strongly related to concepts such as sharpness, contrast and spatial resolution. Therefore, it is considered as an important image quality metric.

(It is important that this image quality metric be monitored post-launch or in orbit, not just pre-launch, in order to ensure that launch vibrations, transitions from air to vacuum, or changes in thermal state, have not degraded the sharpness of the optical imagery).

The products used for this assessment include:

Product 12 and 13 (Panchromatic bands only)

The metadata of these particular products indicate MTF compensation has not been applied (i.e. if it had been applied, we would expect the results to show an improved MTF).

Note these are basic Level 1 products (operator definition given in Section 3.1.1, L0 products are generally not made available externally / publicly) as products generated by higher processing levels commonly include resampling kernels which introduces a smoothing effect and therefore degrades the true MTF.

This assessment has been performed using an open-source tool, validated against third party software, made publicly available at https://github.com/JorgeGIG/MTF_Estimator. The tool, accompanied by detailed documentation that includes information on the algorithm (Slanted-Edge methodology based) used, works in the following way:

1. Select a band and create a shapefile which defines the target edge to be used:
 - a. The target edge must be straight and sharp (a man-made target is more likely to have these features) and defined by uniform high and low reflectance surfaces.
 - b. The target edge must be vertical (i.e. the angle is important). This is an important requirement related to how the algorithm works - if an along track or across-track assessment is needed then the image can be rotated accordingly.
2. Run the tool
 - a. The data in each transect (each image row), defined by the shapefile, is smoothed and then differentiated in order to obtain a coarse estimation of the pixel position of the target edge. The latter estimation is then used to set the initial conditions of the optimisation technique which is used to fit a sigmoid function to the data (as shown in Figure 4-10).

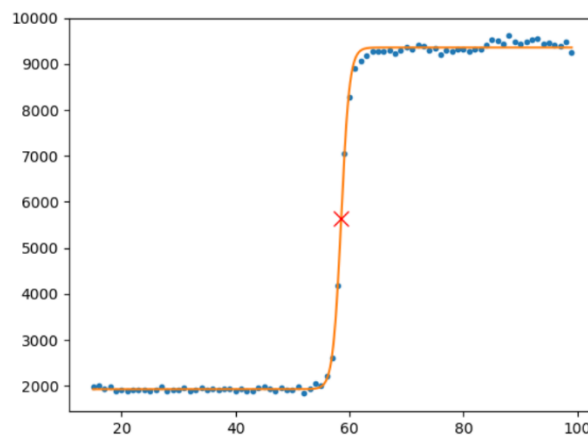


Figure 4-10 The sigmoid function (-) is fitted to the data () in a transect. The point of inflexion (x) shows the estimated sub-pixel edge position. X axis is pixels, y axis is digital numbers

- b. The estimated sub-pixel position data for all transects is subjected to linear regression in order to ensure the target edge is straight as assumed (any outliers are removed during this process) and the target edge angle estimated.
- c. The estimated sub-pixel edge position is used to shift each transect to a common origin, hence creating a supersampled virtual edge which is modelled as a spline and thus a representation of the Edge Spread Function (**ESF**).
- d. The Point Spread Function (**PSF**) is obtained by fitting the spline shape to a Gaussian function (Line Spread Function) using Levenberg-Marquardt optimisation.
 - i. The PSF defines the apparent shape of a point target as it appears in the resulting image: it is therefore directly related to the sharpness of images provided by the sensor / imaging system [RD-14].
- e. The MTF is then estimated from the modulus of the Fourier transform of the PSF.
 - i. The MTF informs on the contrast of the different spatial frequency components of the observed image.

The main disadvantage of this particular method, over some of the other methods, is that sufficient ground target contrast is required (and this is not always easy to find based on issues related to cloud, shadow, target characteristics, etc.). However, irrespective of the method used, the condition of imaging also needs to be taken into consideration: cloud, noise, product processing level, along or across direction of flight, viewing and illumination geometries, storage format, and size of target / spatial resolution relationship (high spatial frequencies correspond to fine image detail).

4.4.2.2 Results

The results of this assessment are included in Figure 4-12 and Figure 4-13.

It was originally intended this assessment be performed using an acquisition of the artificial MTF target located in Salon-de-Provence (ONERA site), commonly used for the calibration / validation of optical VHR sensors, but the tool could not detect the sub-pixel location of the target's edge (see Appendix B). The latter may have been due to (1) the target paint areas are no longer homogenous, due to weathering over time, and therefore requires repainting (planned ESA activity for 2022) and / or (2) the inner edges of the target appear to be affected by an artefact (aliasing?), as evident in Figure 4-11.

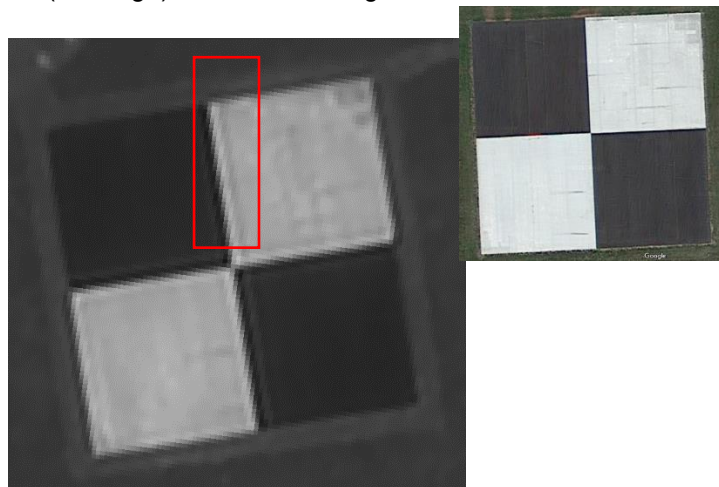


Figure 4-11 The ONERA MTF target from Product 13 (Panchromatic) and Google Maps.

Instead, another two artificial targets, not specifically designed for this type of assessment like the one in Salon-de-Provence, were used and the results are given below.

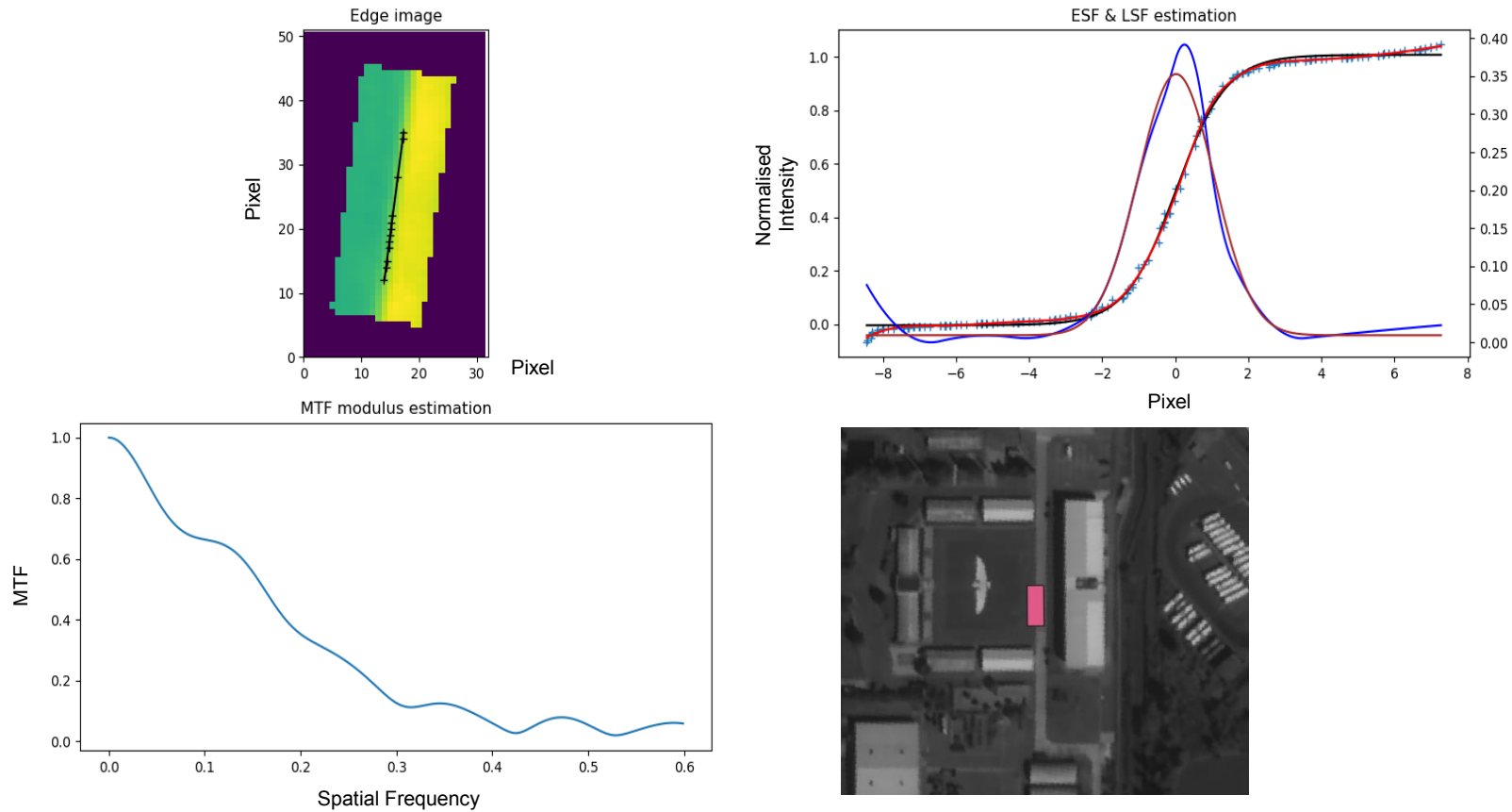


Figure 4-12 MTF assessment using target edge 1 (shapefile, bottom right) in product 12: (top left) transects successfully used to detect the sub-pixel location of the edge (i.e. supersampled edge), (top right) supersampled edge (light blue), the best-fit Gaussian resulting from the optimisation used (brown), optimised ESF spline numeric model (red) and optimised PSF spline numeric model (blue). The (bottom left) the MTF modulus estimation.

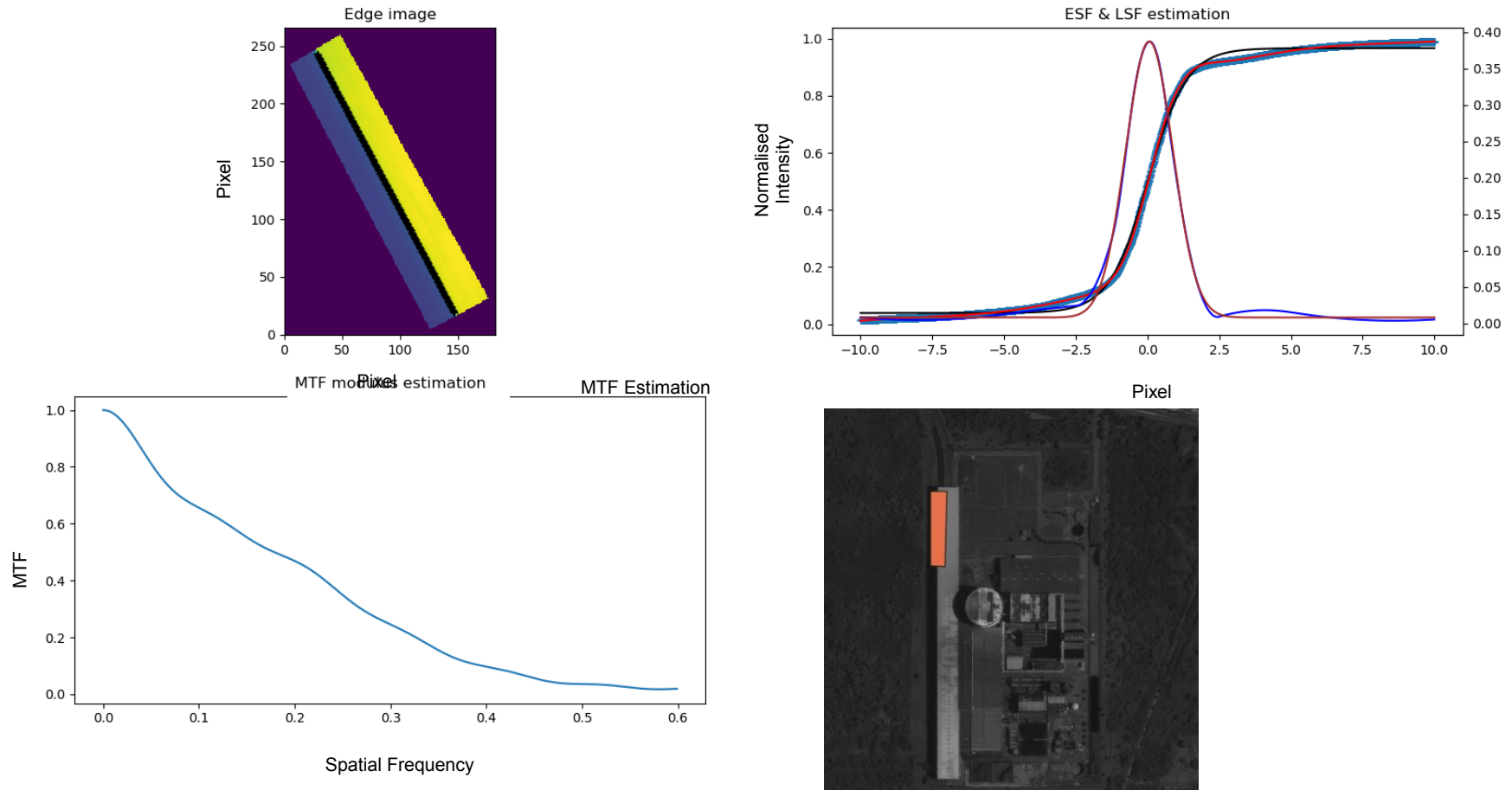


Figure 4-13 MTF assessment using target edge 2 (shapefile, bottom right) in product 12: (top left) transects successfully used to detect the sub-pixel location of the edge (i.e. supersampled edge), (top right) supersampled edge (light blue), the best-fit Gaussian resulting from the optimisation used (brown), optimised ESF spline numeric model (red) and optimised PSF spline numeric model (blue). The (bottom left) the MTF modulus estimation.

Table 4-14 Product 12 (Panchromatic Band) MTF Results

Parameter	Target Edge 1	Target Edge 2
Orientation	- 8.20 °	27.99 °
FWHM	2.45 pixels	1.93 pixels
MTF@N _f	0.05 (5%)	0.04 (4%)

The MTF@N_f of the imagery provided is lower than that defined by the minimum performance requirement specified by the operator in [RD-13], which is panchromatic > 0.16 (Multispectral: >0.28). It is not known if the minimum performance requirement is based on pre-launch or post-launch values.

The sampling period or frequency is usually defined by the ground sampling distance or by the corresponding Nyquist frequency (N_f), which is defined as half the inverse of the ground sampling distance (for example, for KF01B, MS N_f= 0.25 and Pan N_f= 1.0). Given a ground sampling distance, the N_f essentially corresponds to the highest spatial frequency that can be represented by the imaging system [RD-14] (i.e. signals with spatial frequencies higher than N_f cannot be reliably reproduced and can cause aliasing).

4.4.3 Image Interpretability

4.4.3.1 Description and Method

The image interpretability of optical sensor imagery is an important aspect of image quality (originating from the actual sensor or image processing), especially in terms of their practical use or application. This is commonly assessed, subjectively, using a well-defined procedure that is based on the successful interpretation of objects or features according to the National Imagery Interpretability Rating Scale (**NIIRS**) category in which the sensor belongs. This well-defined procedure also importantly allows for the cross-comparison of image quality from similar sensors.

The products used for this assessment are the following:

Product 11, 14

Reference Product: <Pléiades>

The method used to assess image interpretability consists of the visual inspection of suitably sized clips of the sensor's imagery, for all bands, centred on the points (objects or features) of interest listed in Table 4-15. If the latter can be successfully detected, at the very least, then image interpretability is considered as good.

Note comparisons are made with clips from a 'gold standard' reference mission (e.g. Pléiades High-Resolution (**PHR**) imagery (bands 1 – 3 only), following downsampling of the spatial resolution to match the spatial resolution of KF01, also.

The points of interest (**POI**) used for this assessment are deemed suitable for **NIIRS Category 3 (2.5 – 4.5 m)** and **NIIRS Category 5 (0.75 – 1.2 m GSD)** [RD-10] imagery.

Table 4-15 POI in Salon-de-Provence.

wkt_geom (UTM 31)	Id	Description
Point (671090.3105554151115939 4830278.58671295549720526)	1	Modulation Transfer Function target
Point (671364.24309313111007214 4833044.0252351425588131)	2	Motor way / sharp transition (45° NE)
Point (668580.81736886233557016 4828965.45189037173986435)	3	Forest
Point (670056.62237295764498413 4828905.08180973120033741)	4	Roundabout / parking lot
Point (669985.90922565956134349 4832120.72269264236092567)	5	Elevated tree
Point (669956.03863696497865021 4832655.53592716064304113)	6	Motor way / roundabout
Point (670564.24590074480511248 4833363.40447467099875212)	7	The dam
Point (669836.88448120269458741 4832528.00618595350533724)	8	Big building (shadow)
Point (670518.95015854423400015 4829513.56928175128996372)	9	Landing track - 34
Point (670249.72702971810940653 4831735.0312919020652771)	10	Floor painting
Point (670900.38168655894696712 4829617.21182315889745951)	11	Crop fields / sparse
Point (671548.0352310094749555 4830292.1131860688328743)	12	Broad-leaved woodland
Point (671099.93821095407474786 4828090.14610077627003193)	13	Crop fields
Point (671156.44116920174565166 4828825.77096180152148008)	14	Bridge and water
Point (671120.4438803291413933 4827691.31545618735253811)	15	Crop fields
Point (670328.31568091106601059 4831489.30539688002318144)	16	Building / EA 15
Point (671516.86161747551523149 4833207.41657157335430384)	17	Greenhouse
Point (669996.87127304612658918 4829099.09009433817118406)	18	Parking lot
Point (670062.87681329366751015 4829781.35287734866142273)	19	Plane parking
Point (670860.46870227111503482 4831527.10888031311333179)	20	Plane hangar
Point (671246.59432400949299335 4832300.03732818737626076)	22	Urban city

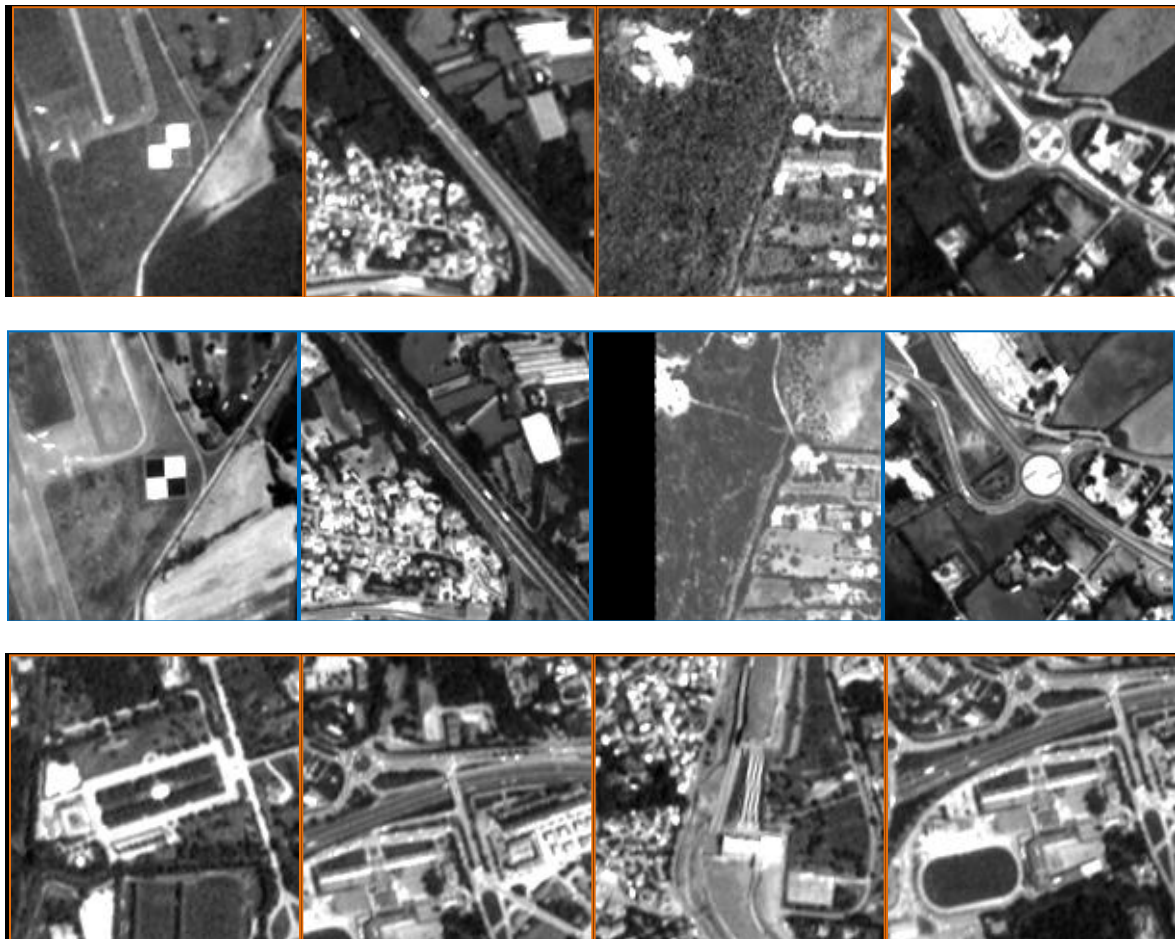
4.4.3.2 Results

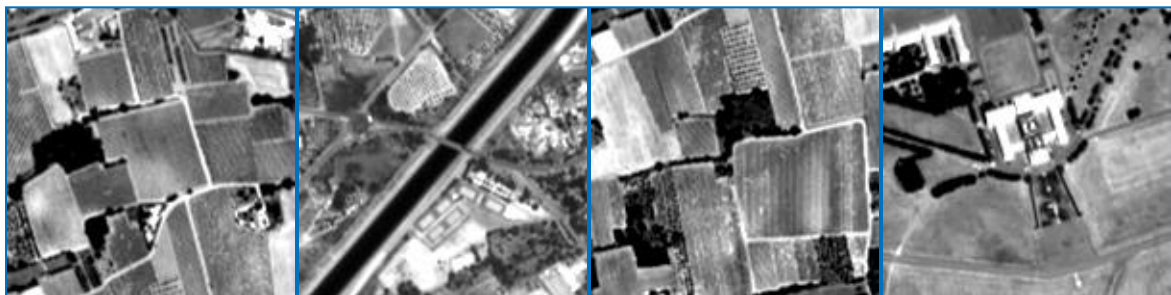
The primary results generally indicate the image interpretability is reasonable as the POI can be delineated in both the multispectral and panchromatic imagery, as shown in the figures below (this could be improved upon with the reduction of blurring, evident and supported by the preliminary assessment detailed in Section 4.4.2).

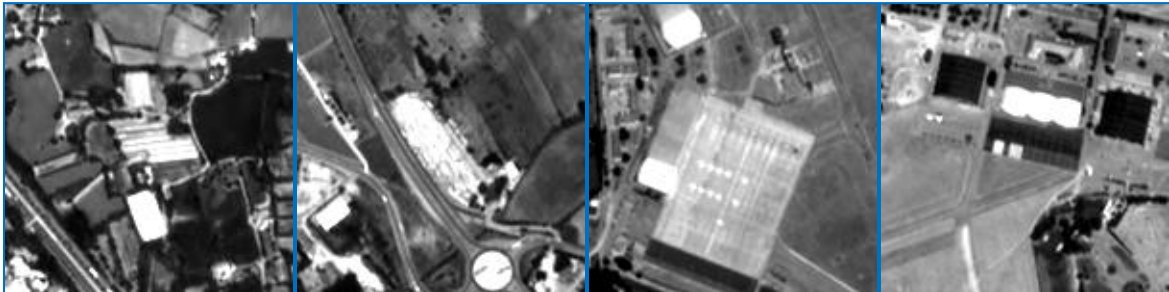
The secondary results generally indicate the image interpretability of KF01A and KF01B is the same (the spatial resolution of panchromatic imagery from KF01B is downsampled to match the spatial resolution of KF01A imagery).

Note this assessment takes into account that the contrast is different between the imagery from the two sensors, which is expected as the two sensors have different spectral characteristics, and so is considered as only a minor disadvantage to using this particular method.

Band 1 (Jilin-1 KF01A, Pléiades, POI 1 - 21)

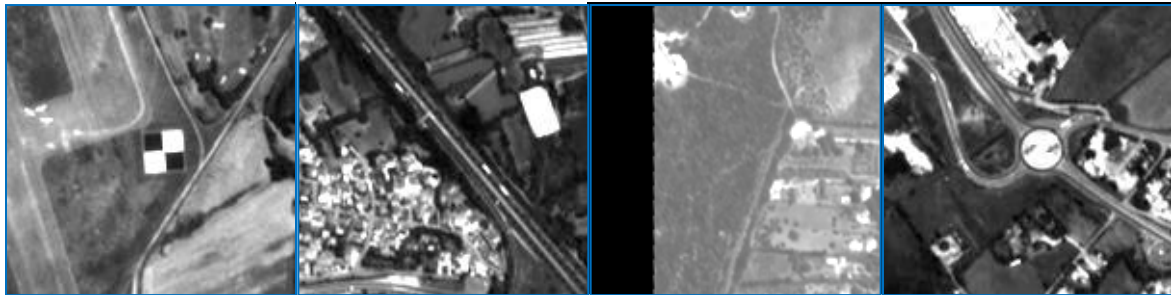






Band 2 (KF01A, Pléiades, POI 1 - 21)

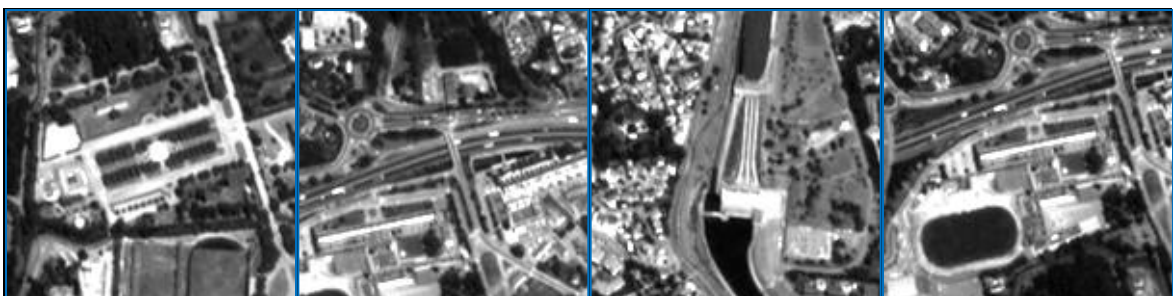
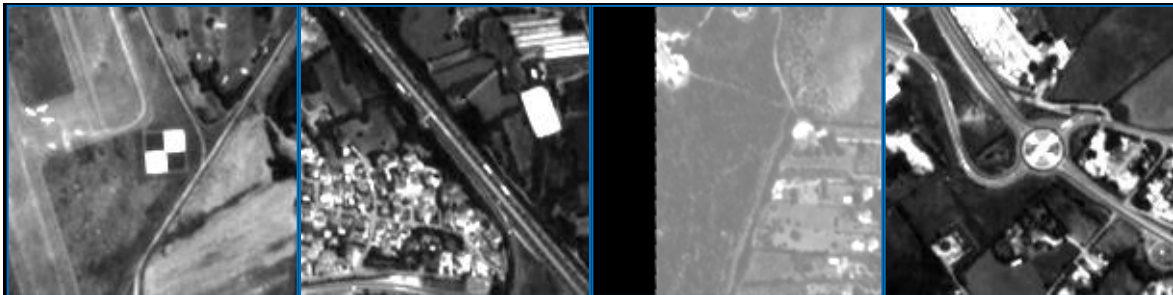
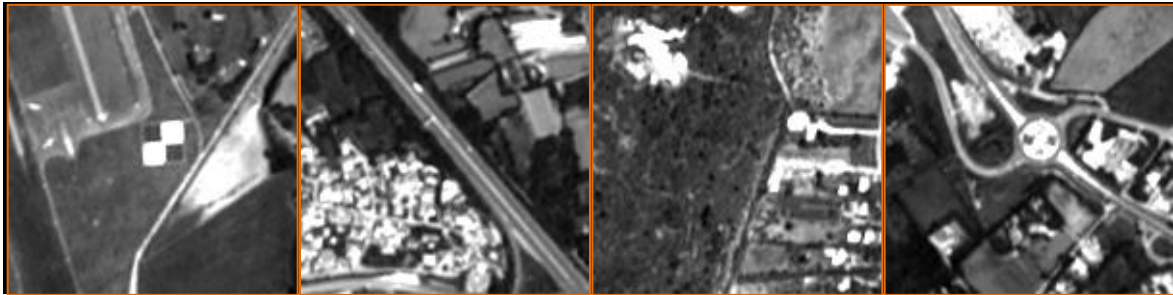


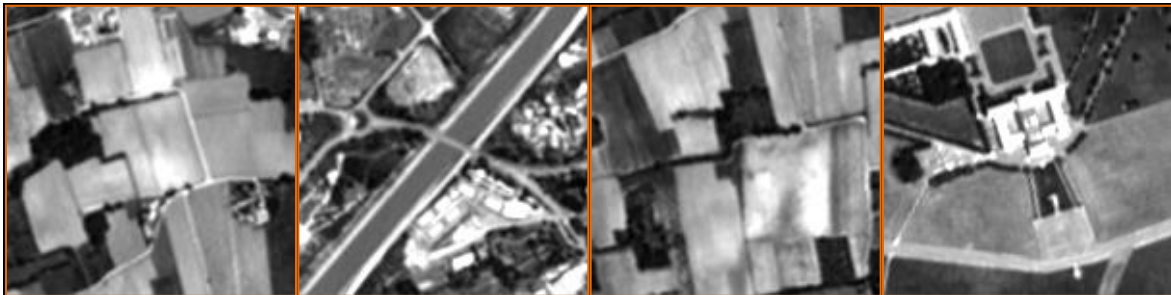






Band 3 (KF01A, Pléiades, POI 1 - 21)

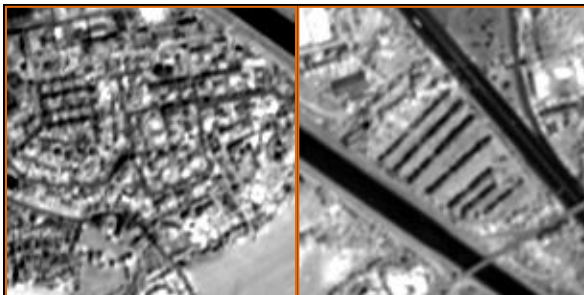




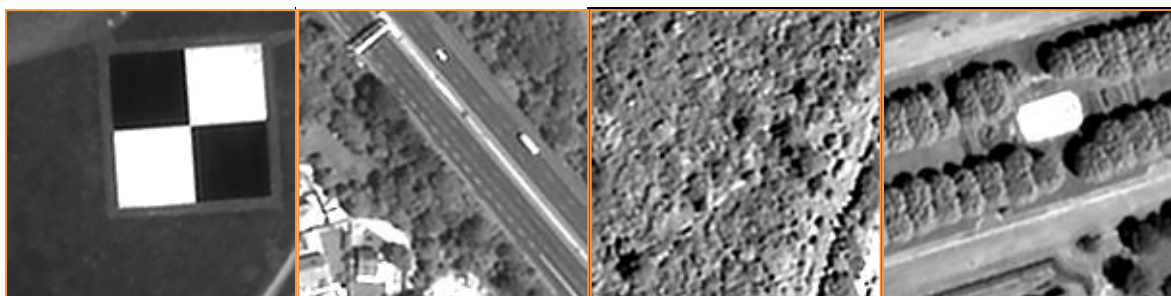


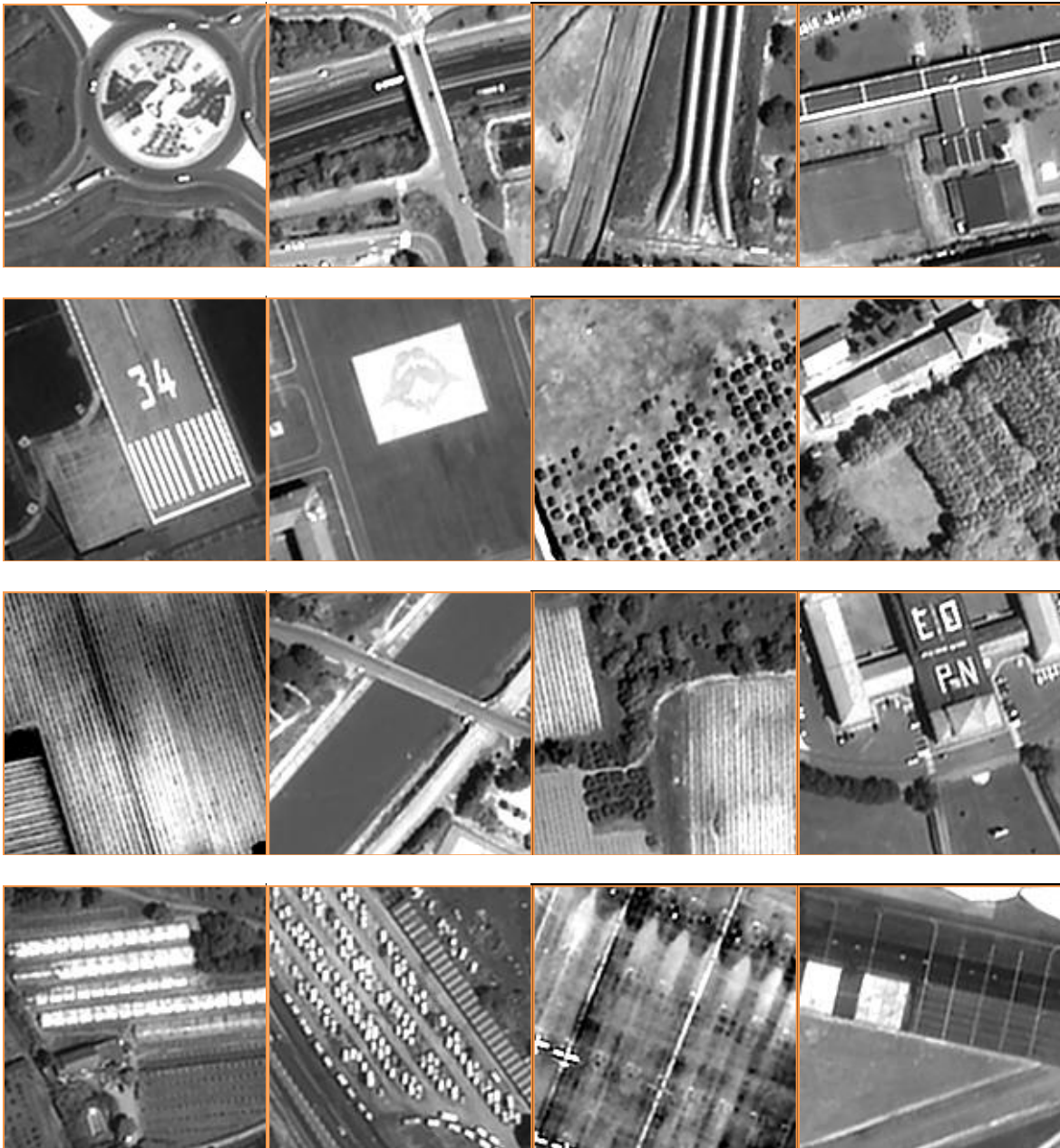
Band 4 (KF01A, POI 1 - 21)

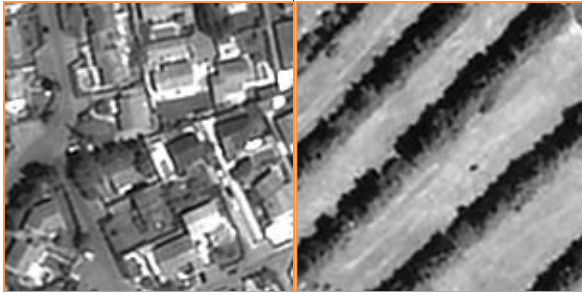




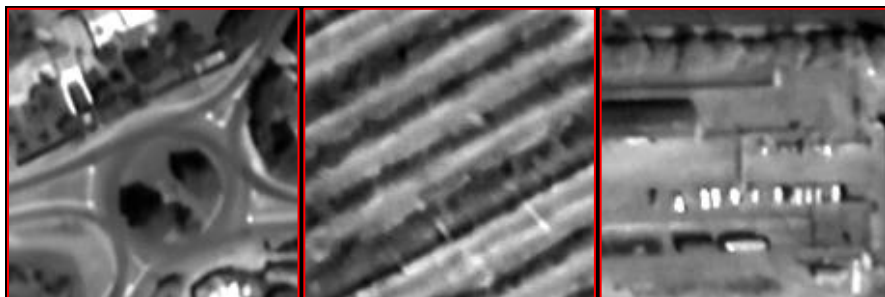
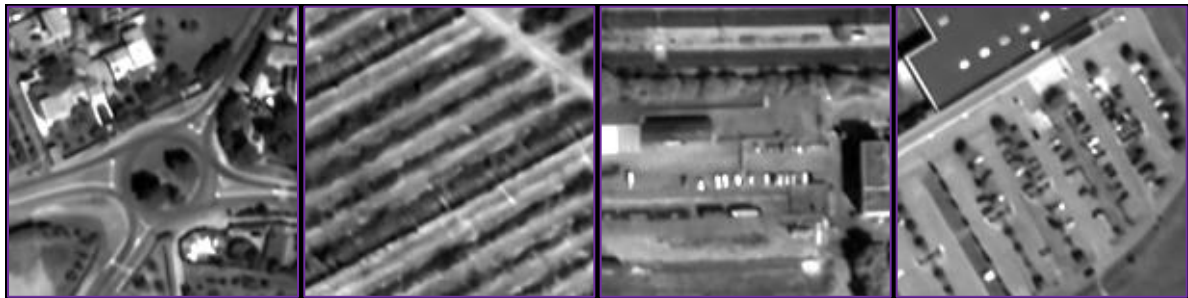
Band PAN (KF01A, POI 1 - 21)







This assessment was repeated in order to produce a comparison of image quality / interpretability between panchromatic imagery (only) from **KF01A**, **KF01B** (downsampled) and **KF01B** (original). The results of this assessment appear to indicate the interpretability of imagery from KF01A is better than KF01B – KF01B appears to be oversmoothed, when compared with KF01A, making it slightly more difficult to delineate the POIs.







4.5 Visual Inspections





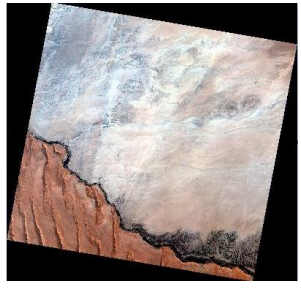
4.5.1 Description and Method

General visual inspections were performed on the multispectral (all bands but only browse image shown below) and panchromatic imagery included in the sample of orthorectified products procured, in order to ensure there were no anomalies or artefacts present. The results are detailed in Section 4.5.2.

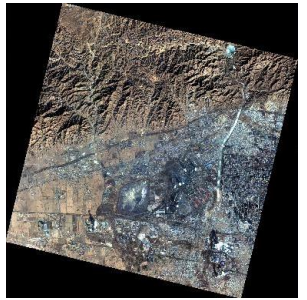
Note the visual inspections of the product imagery also include inspections of their histograms (e.g. support detection of anomalies or artefacts in the imagery, including saturation) and product metadata (the inspection and extraction of relevant metadata, for example the product quality grade and cloud score, for supporting information despite them not being fully described in the documentation (e.g. how is the product quality grade determined)).

4.5.2 Results

Product	Visual Inspection Results	
1	<p>La Crau (France)</p> <p>Product Name: JL1KF01A_PMS04_20200707180240_200027911_103_002 1_001_L3A</p> <p>Product Quality Grade: A</p> <p>Cloud Score: 0 (%)</p> <p>Comment: The imagery does not appear to contain any anomalies or artefacts. The cloud score also appears to be estimated accurately also.</p>	
2	<p>La Crau (France)</p> <p>Product Name: JL1KF01B_PMS05_20210905181026_200060331_103_000 1_001_L3A</p> <p>Product Quality Grade: A</p> <p>Cloud Score: 1 (%)</p> <p>Comment: The imagery does not appear to contain any anomalies or artefacts. The cloud score also appears to be estimated accurately also.</p>	

3	<p>La Crau (France)</p> <p>Product Name: JL1KF01B_PMS05_20210905181026_200060331_103_000_2_001_L3A</p> <p>Product Quality Grade: B</p> <p>Cloud Score: 1 (%)</p> <p>Comment: The imagery does not appear to contain any anomalies or artefacts. The cloud score also appears to be estimated accurately also.</p>	
4	<p>Salon-de-Provence (France)</p> <p>Product Name: JL1KF01A_PMS01_20210615174508_200052889_103_000_2_001_L3A</p> <p>Product Quality Grade: A</p> <p>Cloud Score: 0 (%)</p> <p>Comment: The imagery does not appear to contain any anomalies or artefacts. The cloud score also appears to be estimated accurately also.</p>	
5	<p>Salon-de-Provence (France)</p> <p>Product Name: JL1KF01A_PMS05_20210527175657_200051097_102_000_1_001_L3A</p> <p>Product Quality Grade: A</p> <p>Cloud Score: 0 (%)</p> <p>Comment: The imagery does not appear to contain any anomalies or artefacts. The cloud score also appears to be estimated accurately also.</p>	
6	<p>Gobabeb (Namibia)</p> <p>Product Name: JL1KF01A_PMS01_20210208163646_200040344_102_001_1_001_L3A</p> <p>Product Quality Grade: A</p> <p>Cloud Score: 8 (%)</p> <p>Comment: The imagery does not appear to contain any anomalies or artefacts.</p>	
7	<p>Gobabeb (Namibia)</p> <p>Product Name: JL1KF01A_PMS06_20210527164019_200051099_103_000_1_001_L3A</p> <p>Product Quality Grade: B</p> <p>Cloud Score: 22 (%)</p>	

	<p>Comment: The imagery does not appear to contain any anomalies or artefacts. The cloud score may be overestimated as the very light-coloured surface geology, composed of calcisols and gypsisols, of this area is predominant in this acquisition and might be mistaken for cloud in the calculation of the cloud score.</p> <p>(It is important to mention that this desert, which is known as a unique coastal fog desert, experiences morning fog (caused by cold currents in the Atlantic cooling the air just above the water, and then the winds blowing the cooled air inland and over the hot desert) on a near daily basis but then if this were the case then you would expect to see it cover the orange coloured Namib Sand Sea also.)</p>	
8	<p>Gobabeb (Namibia)</p> <p>Product Name: JL1KF01A_PMS06_20210622163841_200053495_103_0001_001_L3A</p> <p>Product Quality Grade: A</p> <p>Cloud Score: 23 (%)</p> <p>Comment: The imagery does not appear to contain any anomalies or artefacts. The above comment on cloud score applies.</p>	
9	<p>PICS Libya-4 (Libya)</p> <p>Product Name: JL1KF01A_PMS01_20210405162523_200046230_101_0001_001_L3A</p> <p>Product Quality Grade: B</p> <p>Cloud Score: 26 (%)</p> <p>Comment: The imagery does not appear to contain any anomalies or artefacts. The cloud score also appears to be estimated accurately also.</p> <p>(The stretching of the histogram, when generating the quick looks, causes the strange colouring and this is due to the presence of thick cloud and cloud shadow.)</p>	
10	<p>PICS Libya-4 (Libya)</p> <p>Product Name: JL1KF01A_PMS04_20210401163212_200045798_101_0002_001_L3A</p> <p>Product Quality Grade: B</p> <p>Cloud Score: 9 (%)</p> <p>Comment: The imagery does not appear to contain any anomalies or artefacts. The cloud score also appears to be estimated accurately also.</p>	

	<p>Baotou (China)</p> <p>Product Name: JL1KF01A_PMS05_20210202105928_200039598_101_000 4</p> <p>Product Quality Grade: A</p> <p>Cloud Score: 0 (%)</p> <p>Comment: The imagery does not appear to contain any anomalies or artefacts. The cloud score also appears to be estimated accurately also.</p> <p>(This product was not used in any of the assessments as the region of interest lies just outside of the acquisition.)</p>	 A satellite image showing a landscape with a mix of brown and grey tones, likely representing a semi-arid region. The image is tilted and shows some linear features, possibly roads or irrigation canals, cutting through the terrain.
--	--	---

5. CONCLUSIONS

This technical note details the preliminary data quality assessments (including geometric calibration, radiometric calibration and image quality) that were performed on a small sample of **orthorectified Jilin-1 KF01 bundle products**. The results of the aforementioned data quality assessments conclude that the **performance of the sensor and the processing implemented is relatively good**. It is, however, recommended that the data provider / operator address, at the very least, the following:

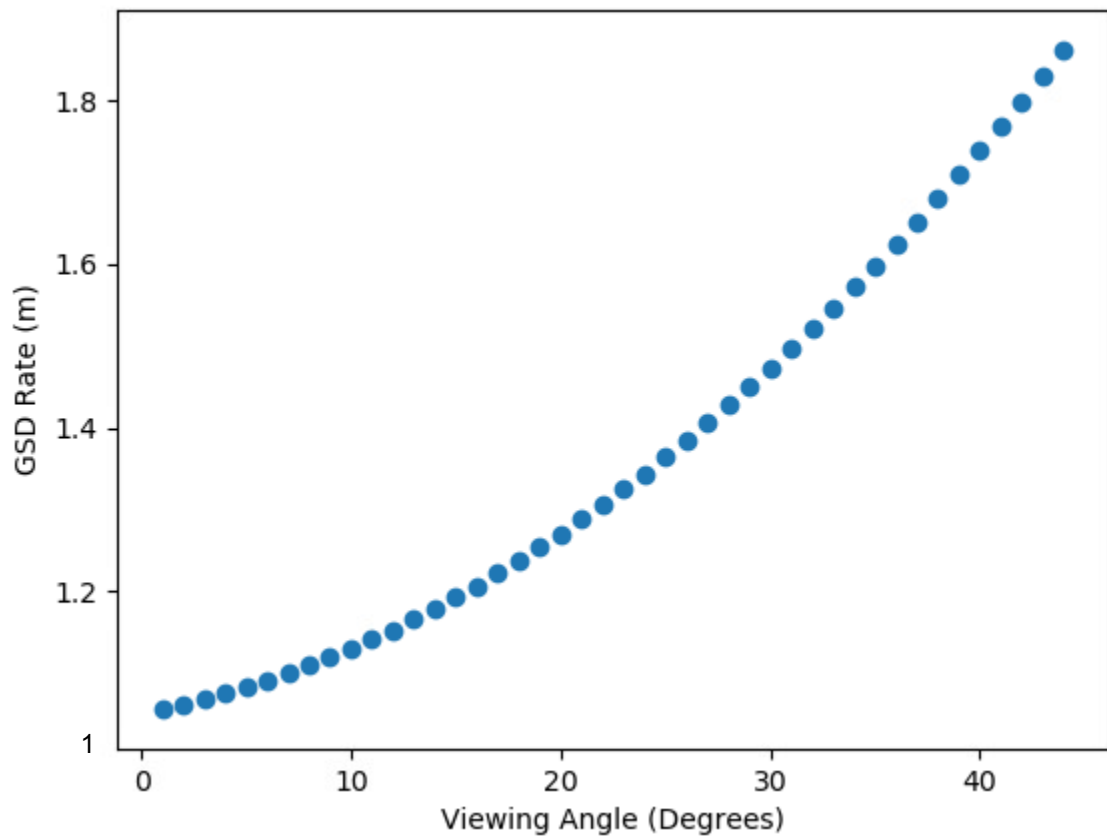
- The provision of more detailed documentation (e.g., the product and quality metadata are a definite asset to the product but, unfortunately, the contents are not adequately described in the user guide and so not all of it can be used reliably or in the correct context).
- The provision of more accurate metadata (currently nadir viewing only) – for a sensor with such a large swath width, this is needed in order to ensure the data is assessed, or processed further, correctly / accurately.
- The provision of all minimum performance requirements so that it is clear to users what level of quality, especially geometrically and radiometrically, can be guaranteed or expected.
- The method used for radiometric calibration should be re-assessed by the operator, for the reasons described in relevant section of this technical note.

Please note the very small sample of products assessed meant that that no comments could be made on items such as the general stability (temporal assessments) or consistency across both satellites.

APPENDIX A GSD ASSESSMENT

The plot below demonstrates how the true ground sampling distance changes for this sensor with increasing viewing angle (or distance from nadir); the plot shows that the true ground sampling distance changes exponentially, and in the most extreme case it increases by just over 80 % at 45° (e.g. 10 % increase at 10°, 50 % at 30°). Therefore, it is important users consider such viewing conditions when assessing / using the data (especially for a sensor with such a large swath width as this one).

This plot was generated using the information provided in [RD-16].



APPENDIX B MTF

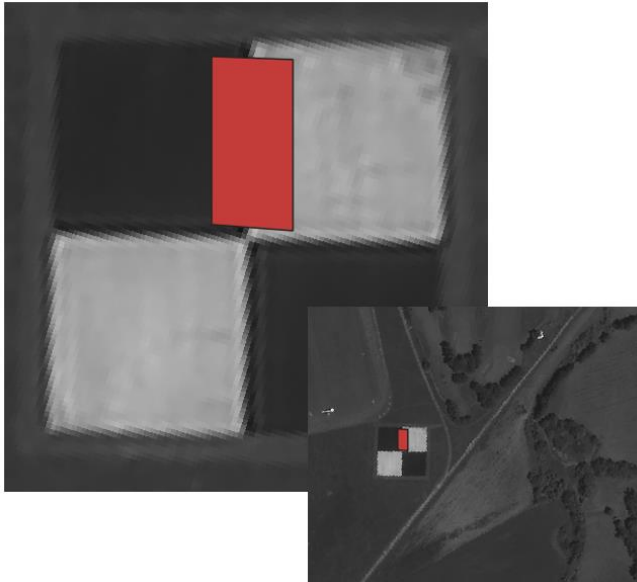


Figure 5-1 The rectangular region of interest, containing the knife-edge provided by the well-known artificial checkerboard (2 x 2, 60 m x 60 m) target located in Salon-de-Provence (commonly used to calibrate VHR sensors, maintained by ONERA), is selected from the panchromatic imagery of Product 13 for this assessment.

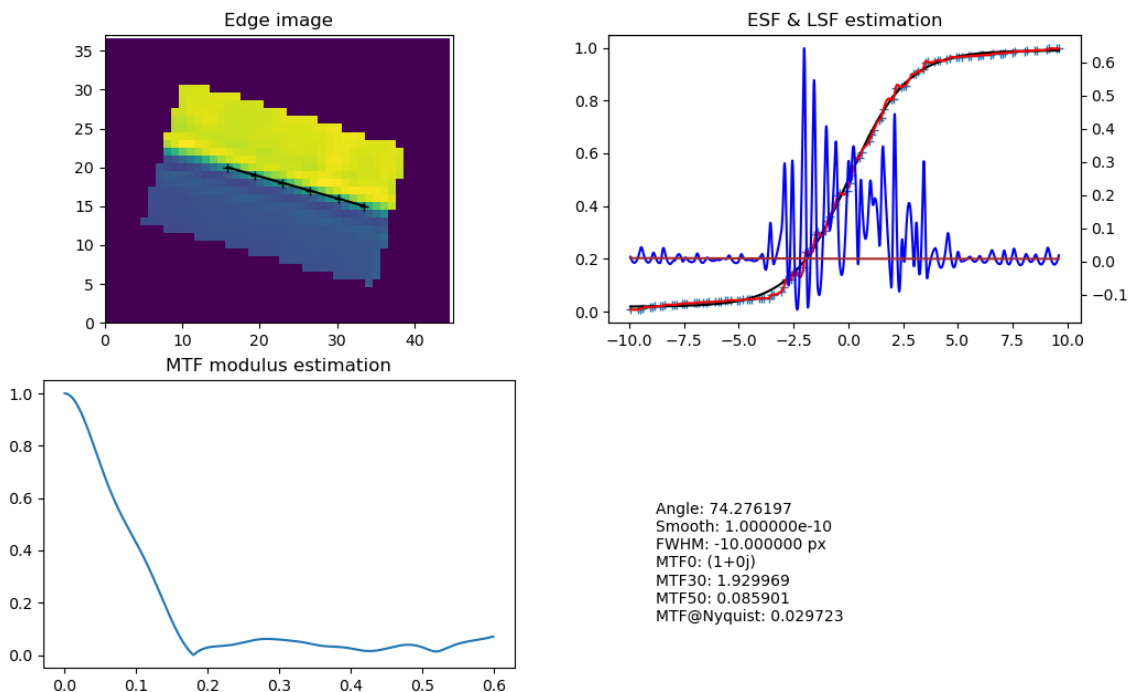


Figure 5-2 The (top left) transects successfully used to detect the sub-pixel location of the edge (i.e. supersampled edge) and the (top right) supersampled edge (light blue), the best-fit Gaussian resulting from the optimisation used, optimised edge-spread function (ESF) spline numeric model (red) and optimised PSF spline numeric model (blue). The (bottom left) the MTF modulus estimation and (bottom right) the numerical results of the assessment on Product 13.

APPENDIX C Jilin-1 KF01A/B TEST DATASET

Site	Product_Identifier (L1 and L3A)
La Crau (France)	JL1KF01A_PMS04_20200707180240_200027911_103_0021_001
La Crau (France)	JL1KF01B_PMS05_20210905181026_200060331_103_0001_001
La Crau (France)	JL1KF01B_PMS05_20210905181026_200060331_103_0002_001
Libya-4 (Libya)	JL1KF01A_PMS01_20210405162523_200046230_101_0001_001
Libya-4 (Libya)	JL1KF01A_PMS04_20210401163212_200045798_101_0002_001
Gobabeb (Namibia)	JL1KF01A_PMS01_20210208163646_200040344_102_0011_001
Gobabeb (Namibia)	JL1KF01A_PMS06_20210527164019_200051099_103_0001_001
Gobabeb (Namibia)	JL1KF01A_PMS06_20210622163841_200053495_103_0001_001
Salon-de-Provence (France)	JL1KF01A_PMS01_20210615174508_200052889_103_0002_001
Salon-de-Provence (France)	JL1KF01A_PMS05_20210527175657_200051097_102_0001_001



[END OF DOCUMENT]